

# Chapter 14

## How the Optical Properties of Leaves Modify the Absorption and Scattering of Energy and Enhance Leaf Functionality



Susan L. Ustin and Stéphane Jacquemoud

### 14.1 Introduction

Leaves interact with light in ways that create a spectral footprint of the terrestrial environment of our planet. Most of the visible light penetrating the Earth's atmosphere is absorbed by leaves, and at wavelengths around 700 nm, just beyond the red visible bands, this pattern abruptly reverses, to reflect about half of the incoming light from 700 to 1000 nm. This region of rapid change in reflectance is termed the "red edge" and produces a distinct pattern in which the Earth's albedo is brighter for wavelengths longer than the red edge than for shorter wavelengths (Arnold et al. 2002; Montañés-Rodríguez et al. 2006). This pattern is a result of the abundance of green leaves in the terrestrial environment absorbing light for photosynthesis, with the red edge the manifestation of the long wavelength edge of chlorophyll pigment absorption. This is one example of how leaf optical properties (the absorption and scattering of different wavelengths of sunlight) permit detection of leaf functional properties.

Because the primary physiological processes and functional properties of seed plants are homologous, evolutionary constraints have optimized physiological properties (Jacquemoud and Ustin 2008; Ustin and Gamon 2010). This means that among higher plant species, concentrations of individual biochemicals in the suite of major biochemicals may vary. So considering overall biochemical traits, different species

---

S. L. Ustin (✉)

Department of Land, Air and Water Resources, University of California Davis,  
Davis, CA, USA

e-mail: [slustin@ucdavis.edu](mailto:slustin@ucdavis.edu)

S. Jacquemoud

Institut de Physique du Globe de Paris – Sorbonne Paris Cité, 8 Université of Paris Diderot,  
Paris, France

e-mail: [jacquemoud@ipgp.jussieu.fr](mailto:jacquemoud@ipgp.jussieu.fr)

© The Author(s) 2020

J. Cavender-Bares et al. (eds.), *Remote Sensing of Plant Biodiversity*,  
[https://doi.org/10.1007/978-3-030-33157-3\\_14](https://doi.org/10.1007/978-3-030-33157-3_14)

349

may have different concentrations of biochemicals that together produce a distinct pattern. Minor biochemicals, such as specific defensive compounds, may reveal more about biodiversity by their presence or absence than by their concentrations.

In their paper on the worldwide leaf economics spectrum, Wright et al. (2004) showed that plant investments in leaf traits represent long-term adaptations to climate characteristics such as length of the growing season, air temperature, and precipitation. Global research on the concept of relating leaf traits to ecosystem functionality (e.g., Wright et al. 2005; Ordoñez et al. 2009; Kattge et al. 2011) and the use of these properties to better understand functional adaptations has rapidly expanded.

In recent years, there has been strong interest in using optical properties to elucidate biodiversity patterns, and identification of functional traits with phylogenetic associations has become a key new objective of spectroscopy and remote sensing (RS) (Martin, Chap. 5; Meireles et al. Chap. 7. With rapid losses of biodiversity, there is a need to improve understanding, identify hot spots, and predict how patterns of biodiversity may change in the future. This has led to renewed interest in whether the optical properties of plants can be understood in a phylogenetic context as well as their functional processes.

## 14.2 On the Optical Spectrum of Seed Plants

There are many definitions of what constitutes the optical spectrum. Most narrowly, it is visible light—the part of the electromagnetic spectrum that can be seen by the human eye (wavelengths 400–700 nm). The full solar spectrum includes all the wavelengths of electromagnetic energy from the sun that reach the Earth's surface. These wavelengths start in the zone of ultraviolet (UV) A (generally longer than 370 nm) and include visible light, near-infrared (NIR, 700–1000 nm), and shortwave-infrared (SWIR, 1000–3000 nm, also termed middle-infrared in some disciplines). Solar energy interacts with a leaf across the full range of wavelengths to produce the leaf's optical properties, which are determined by its biochemical and biophysical characteristics. In recent years, with improved detector technology, it has become possible to measure reflected sunlight with satellite and airborne imagers that have sufficient spectral resolution to access the absorption patterns of an increasing number of chemical compounds. It is the variation in the full suite of chemistry and scattering properties that allows identification of plant species from their leaf spectra—the patterns of absorption and reflection across all wavelengths that can be measured in the solar spectrum.

Seed plants have three basic types of leaves. Monocot and dicot leaves of angiosperms typically have a wide blade, and conifers have needle-shaped leaves. Figure 14.1 shows examples of typical spectra of evergreen (*Quercus wislizeni*) and deciduous (*Quercus douglasii*) dicot leaves, deciduous leaves of a monocot (*Zea mays*), and evergreen conifer needles (*Pinus ponderosa*). The overall shape of the leaf spectra is similar, with low reflectance across visible wavelengths due to absorption by photosynthetic pigments (Gates et al. 1965). High reflectance is

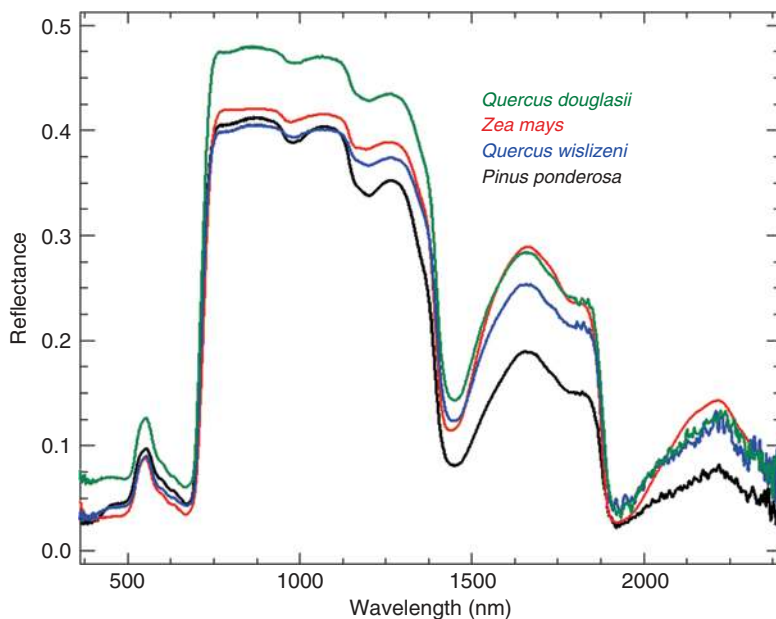


**Fig. 14.1** Typical leaf spectra of evergreen and deciduous species, measured on field-grown leaves in June. *Quercus douglasii* (blue oak) is a deciduous dicot species, *Zea mays* (corn) is a deciduous monocot, *Q. wislizeni* (black oak) is an evergreen dicot species, and *Pinus ponderosa* (ponderosa pine) is a needle-leaf conifer

characteristic of the NIR, where generally 10% or less of radiation is absorbed (Jacquemoud and Ustin 2008); intermediate reflectance is characteristic of the SWIR region (1500–2500 nm), where energy is primarily absorbed by water in leaves (Carter 1991) or by plant residues when leaves are dry. Cell wall compounds such as cellulose and lignin or other biochemicals found in the cytoplasm such as proteins and sugars account for many overlapping absorption features in the SWIR.

Differences between spectra in Fig. 14.1 relate to differences in biochemical composition and concentration of pigments, water, and cell wall structural materials or are due to the sources of scattering at either the leaf surface or from internal cellular structures. Despite the similarity of overall shape, Fig. 14.1 clearly shows tax-specific differences in reflectance across the spectrum. These differences at the leaf scale contribute to our ability to map land cover types and distinguish plant communities, genera, and species, as discussed in other chapters in this book.

Regardless of the diversity in leaf anatomy and morphology, biochemical and biophysical properties exhibit consistent absorption features in the optical spectrum and have been detected in modern high-fidelity airborne imaging spectrometers (e.g., Kokaly et al. 2009; Ustin et al. 2009; Féret et al. 2011; Asner and Martin 2016; Asner et al. 2015). The principles of spectroscopy indicate that many of the chemical compounds with absorption features in the solar spectrum (280–3000 nm) can be detected and identified based on their spectral reflectance features. Both

differences in the amount of energy absorbed and the anatomical and morphological differences that enhance scattering of light at different wavelengths allow us to differentiate related taxa. While this chapter is focused on the leaf scale, complications arise at larger scales; even when just scaling to the canopy, it can be difficult to detect leaf optical properties due to the presence of additional materials adding to the measured spectrum (e.g., live and dead leaves, flowers, fruit, bark, and understory, both vegetation and soil). However, in some cases, if the absorptivity of the material is weak, the absorption at the canopy [pixel] scale can be enhanced. An example of this is observed for foliar water content when measured on a single leaf or a spectrum from multiple leaves (e.g., Roberts et al. 2004; Kokaly et al. 2009). Our ability to measure leaf optical properties from airborne and satellite sensors varies with spatial scales, as discussed in Chap. 16.

### 14.3 Leaf Reflectance Patterns

Reflectance is the fraction of light reflected from the leaf surface ( $R_s$ ). It is composed of two parts: specular reflectance, which reflects directly off the surface in the forward direction, and diffuse reflectance, which scatters light in all directions from the surface. Light can be specularly scattered at some wavelengths and diffusely scattered at others, depending on the scale of the roughness of the surface. Specular reflectance happens when light intersects a surface that is smooth, i.e., one with particles much smaller than the wavelengths contacting it. If the surface is rough, that is, composed of particles about the size of the wavelengths of light or larger, it will scatter light diffusely. Specular reflection is a leaf property that is determined by the structure and chemical composition of the cuticle; thus, differences among species are potentially related to biodiversity questions.

The fraction of light that is reflected from the interior of the leaf,  $R_i$ , is the diffuse or multiply scattered component. Some fraction of the beam of light that enters the leaf's interior will be absorbed, some transmitted through the leaf, and some will be scattered back out of the upper surface of the leaf. Only the fraction of the incident light that is reflected from the interior of the leaf carries information about the biochemical and structural properties of the leaf.

Reflectance patterns in the visible spectrum are primarily due to photosynthetic pigments that absorb about 90% or more of the incoming light (Gates et al. 1965). Water is the second strongest absorbing molecule in leaves; it absorbs strongly in the SWIR region, with several smaller vibrational overtone absorptions in the NIR (Carter 1991). Because there are no strongly absorbing molecules in the NIR, plants reflect or transmit all but about 10% of the incoming radiation in this region (Jacquemoud and Ustin 2008).

While the spectral shapes of leaves are generally consistent across all green plants, they differ between species and plant functional types. Evergreen leaves usually have thicker cell walls and smaller cells and are more compact than deciduous leaves. Consequently, their spectral signatures generally have lower reflectance in

the NIR and SWIR (Fig. 14.1). Phenological changes over the growing season are expressed in leaf reflectance by declining pigment and water contents and increases in the mass of secondary cell wall components as the growing season nears its end. Similar patterns are also observed when comparing leaves from mesic to arid habitats.

In late spring, when the leaves shown in Fig. 14.1 were measured, phenological differences are generally minimized because leaves are near their growth peak. The leaves in Fig. 14.1 show they have high water content as the water absorption features in the NIR, around 970 nm and 1240 nm, are relatively deep for non-succulent leaves. Water causes absorption at all wavelengths longer than 1400 nm, decreasing reflectance across the spectrum. The small absorption feature observed near 1800 nm is from cellulose and other related structural C (C) compounds. In addition to these few large absorption features, many small absorptions exist, only some of which are identified with a specific biochemical. The wide variety of secondary biochemicals that exist in plant leaves and their possible range of concentrations provides a spectral palette that can be used to identify individual species in optical data.

Clearly, the environmental conditions that a plant is exposed to, including soil properties, weather, and its phenological age, alter the leaf's optical properties. The genetic heritage modulates the types of responses of a species to environmental conditions. The reflection of light from the leaf and transmission through the leaf are determined by what wavelengths of light are absorbed by the various biochemical compounds in leaves (chlorophylls, carotenoids, water, cellulose and lignin, proteins, etc.) and the relative strength of the absorptions.

The scattering of light at the leaf surface depends on the structure of the epidermis, the waxes, cutin, and protrusions such as leaf hairs (Ehleringer et al. 1976) and on the orientation of the leaf to the beam of light (Comstock and Mahall 1985; James and Bell 2000). The variety of leaf properties are expressions of different adaptive strategies among species and are related to their functional traits (Serbin and Townsend, Chap. 3). For example, differences in epidermal structure cause leaves of one species to have a bluish powder coating, those of a different species to appear white, and those of another to have a shiny smooth green surface.

Within the leaf, scattering occurs between cells and between organelles within cells (Vogelmann 1993). Vogelmann et al. (1996a) used fiber optics to study scattering processes within cells and tissues to show how leaf anatomy modifies the internal light environment to optimize photosynthetic performance under different habitat conditions.

## 14.4 Leaf Transmittance Patterns

Transmittance is the fraction of light that enters a leaf and is eventually scattered out the opposite surface. The transmittance spectrum approximates the reflectance spectrum, but they are not exact copies of each other. Transmittance can be greater

or lesser than reflectance (Knipling 1970; Wooley 1971; Jacquemoud and Ustin 2008), depending on leaf thickness, number of leaves light passes through, and their optical properties. Thus, transmittance spectra carry information about leaf traits and biodiversity but are seldom used in remote sensing (RS) except in field-based or laboratory studies.

## 14.5 Leaf Absorptance Patterns

The absorption of light is determined by the absorbing molecules in the leaf balanced by the structural properties that scatter light, such as air spaces and water–air interfaces. In the visible spectrum, it is photosynthetic pigments, primarily chlorophylls and carotenoids that strongly absorb light. Other non-photosynthetic pigments also absorb in this wavelength region, such as anthocyanins (a large and diverse group of flavonoids that are involved with leaf color but also colors of flowers and fruit). Anthocyanins (and more generally flavonoids) provide photoprotection from UV light (Stapleton 1992; Steyn et al. 2002), such as in alpine environments or during early leaf development (Chalker-Scott 1999; Karageorgou and Manetas 2006) when the photosynthetic machinery is not fully developed. Figure 14.2 shows two adjacent evergreen shrubs in early spring, both widely planted cultivars, one (*Photinia x fraseri*) with red expanding leaves and the other (*Xylosma congesta*) with orange colored expanding leaves. Such differences could indicate pH differences in the vacuoles or different combinations of anthocyanin pigments, or combinations of anthocyanin and carotenoid pigments. Lee and Collins

**Fig. 14.2** Red and orange expanding leaves on adjacent shrubs. Color differences could represent different anthocyanin molecules, different pH environments in the vacuoles, or a mixture of carotenoid and anthocyanin pigments





(2001) evaluated leaf ontogeny and found that spring leaf expansion was usually correlated with high anthocyanin pigments in the mesophyll tissue. Along with phenolic compounds, anthocyanins provide protection of the pigment molecules during senescence (Matile 2000) and defensive functions against herbivory (Hamilton and Brown 2001) and during leaf senescence. Some molecules absorb in the UV and blue wavelengths, ranging from the simplest phenol to complex polyphenols like tannic acid. Kokaly and Skidmore (2015) recently demonstrated detection of a phenolic absorption in plants at 1660 nm. Phenolic compounds often provide regulatory and defensive functions. Because of the great diversity of non-photosynthetic pigments and photosynthetic accessory pigments (carotenoids), pigments provide a basis for discriminating among plant species in optical data. Suites of pigments often occur in specific families or clades in agreement with molecular phylogeny (Lee and Collins 2001).

In the NIR, there are no strongly absorbing compounds, so a high proportion of light is reflected or transmitted. Light is often scattered multiple times, increasing the probability of absorption before being reflected or transmitted out of the leaf. For example, Wooley (1971) reported 4% NIR absorbance in soybean (*Glycine max*), and Everitt et al. (1985) found only 5% NIR absorbance in buffalo grass (*Bouteloua dactyloides*) leaves. Scattering within the leaf is related to the internal cellular structure, especially at cell membrane and air interfaces, where light can be reflected and refracted. Allen et al. (1970) showed the volume of intercellular air spaces was highly correlated with NIR reflectance. Multiple scattering of photons causes the NIR reflectance to be much higher than reflectance of visible or SWIR wavelengths, where absorptions by pigments and water result in single scattering processes (light is absorbed or scattered on its first interaction).

Secondary water absorption features in leaves are found around 980 nm and 1240 nm (Carter 1991). The diversity of plant adaptations to different water regimes results in a wide range of leaf water contents among species. The percent water content is generally positively correlated with increasing leaf thickness, but the opposite may occur. Thus, a sclerophyllous leaf species like *Adenostoma fasciculatum* (chamise) can have higher leaf mass area (LMA = 1 divided by specific leaf area) and low water content, but a succulent species may have high water content and a high leaf mass per area (Ackerly et al. 2002; Vendramaini et al. 2002).

The SWIR part of the leaf spectrum is dominated by water absorption when the leaves are living and by leaf chemical constituents when dry. Many plant compounds have absorptions in the SWIR, including cellulose, lignin, nitrogen (N), sugars, starch, and waxes. Interpretation of these absorption features in dry leaves is complicated because many molecules have absorptions at overlapping wavelengths and we lack the specific absorption coefficients to identify them in the data. The cell wall C compounds comprise the largest fraction of the dry biomass of a leaf, and the absorption feature around 1750 nm is generally attributed to these materials (Kokaly et al. 2009). Kokaly (2001) also identified two absorptions at 2054 nm and 2172 nm that cause broadening of the 2100 nm absorption feature due to N compounds. The complexity of relationships among species adaptations for water, structural carbohydrates, and nutrients provides a strong basis for detecting species diversity in RS imagery, at least in local to regional studies (Asner and Martin 2016).

## 14.6 Physical Processes Underlying Leaf Optical Properties

Leaf anatomy and phylogeny determine how leaf cells (epidermis, mesophyll) and specialized tissues (xylem and phloem conducting tissues and the stomatal complex) are arranged (Al-Edany and Al-Saadi 2012) and how this affects reflectance. There are many modifications, but the standard arrangement of cells and tissues in dicot plants is strongly asymmetric, commonly flattened in the dorsiventral orientation with the adaxial side of the leaf oriented upward (Fig. 14.3). This places the chloroplast-rich palisade parenchyma near the upper surface to intercept incoming light and the spongy mesophyll and large air spaces on the abaxial side of the leaf near the lower surface where all or most of the stomata are located. Clearly, this bifacial arrangement is adapted to facilitate gas exchange and photosynthesis (Parkhurst 1986). Leaves on plants grown under high light tend to have more compact parenchyma than leaves in low light environments, which have more air spaces.

In another common arrangement, grass leaves are isobilateral with the interior of the leaf filled with generalized mesophyll parenchyma cells and stomata on both surfaces. Conifer needles are more cylindrical with the interior filled with generalized parenchyma cells and a central vascular bundle, separated from the mesophyll by an endodermal cell layer. Conifer needles are compact, with little air space between cells. This reduces the interior scattering of light within leaves and contributes to the low NIR reflectance of conifer needles compared with broadleaf plants.

Another leaf type has symmetrical palisade parenchyma on both the top and bottom of the leaf. This is common in dicot species with extreme erectophile leaf orientation, such as the hanging adult leaves of eucalyptus species such as *Eucalyptus*

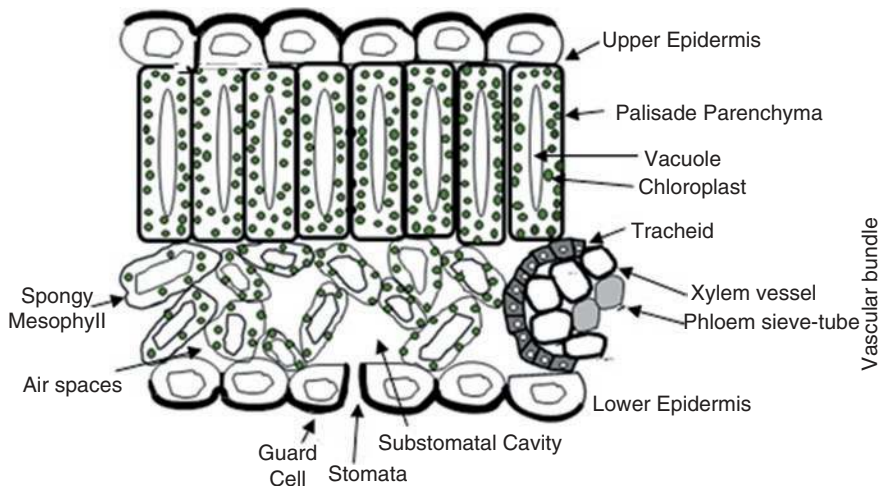


**Fig. 14.3** Dorsiventral cross section of a dicot leaf with the adaxial surface at the top. This is the most common structure of dicot leaves, with a distinct asymmetry oriented toward incoming light from the adaxial surface



*nitens*. The more rounded juvenile leaves of this species have larger air spaces than the adult leaves, suggesting they may be adapted to more rapid growth but have less tolerance to drought (Gras et al. 2005). This type of adult leaf anatomy increases light interception at lower solar zenith angles closer to sunrise and sunset and enhances potential for photosynthesis.

The asymmetric leaf structure of typical dicots enhances capture of energy for photosynthesis by orienting the leaf upright, facilitated by branching angle and petiole orientation. It makes a difference whether light enters the leaf from the upper or lower surfaces because the anatomical structures and biochemistry across the leaf are different. The effect of the asymmetric distribution on reflectance and absorbance patterns is shown in Fig. 14.4 for photosynthetic light at two solar zenith angles entering the leaf from the upper or lower side of the leaf.

The downward flux constitutes most of the net flux when the solar zenith angle is higher (left side); when the solar zenith angle is lower (right side), the upward flux is much larger. The panel (14.4. #1 and 14.4. #2) with the typical dorsiventral orientation has higher net flux through the epidermis than panels (14.4. #3 and 14.4. #4) with the abaxial side receiving the incident flux. About 20% of the net flux enters the palisade parenchyma in 14.4. #1 and 14.4. #2, while 14.4.#3 and 14.4. #4 show very low net flux. Because the chlorophyll concentration is highest in the palisade parenchyma, comparatively little photosynthesis occurs in the spongy mesophyll, with higher net flux of 675 nm light (suitable for chlorophyll a absorption in photosystem II).

Panel 14.4. #1, with the typical dorsiventral orientation (adaxial side up) at the higher solar zenith angle, has higher net flux downward (about 20%) through the epidermis than Panel 14.4. #2 with the lower solar zenith angle, where the net flux is much lower in both palisade and spongy parenchyma and the upward flux is much larger. Panel 14.4. #3, with the abaxial side up, shows little difference in upward flux, but most of the net flux continues to be located in the palisade parenchyma. Panel 14.4. #4, with the abaxial side receiving the light at the lower zenith angle, has virtually no net flux into the palisade parenchyma and high upward flux in the abaxial epidermis. Because the chlorophyll concentration is highest in the palisade parenchyma, there is little photosynthesis elsewhere, even with high net flux of 675 nm light (red wavelength region, suitable for chlorophyll *a* absorption).

## 14.7 The Epidermis

The epidermis is the outermost layer of leaf cells and is generally one cell layer thick, but some species have several cell layers. The epidermis lacks pigments and is generally transparent to light. The outer cuticle surface is covered by wax to limit uptake and loss of gases, except at the stomatal complexes, which are generally located on the abaxial (lower) side of the leaf. Stomata are composed of two kidney-shaped stomatal cells and two to four guard cells at the ends. The stomata are generally located above an open space in the mesophyll where gases can collect, termed

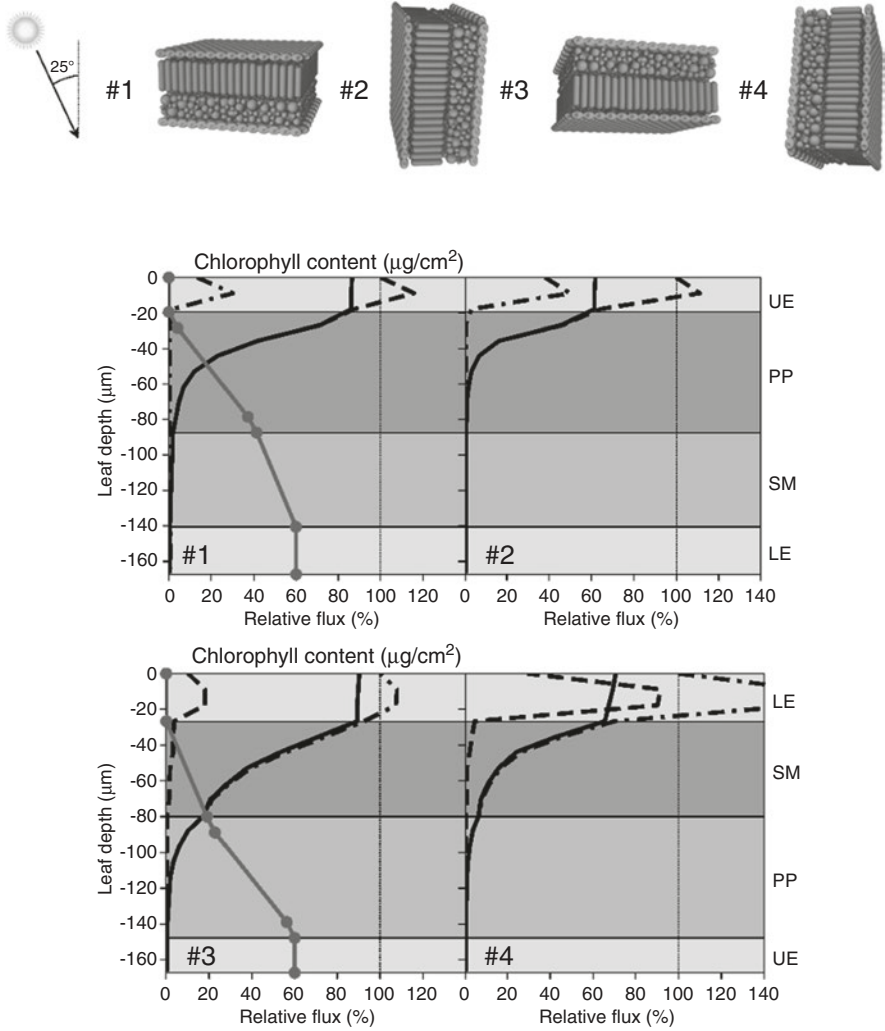


**Fig. 14.4** Top panel illustrates the four orientations selected to simulate the absorption profiles of a dicot leaf. Lower panels show the distribution of relative downward flux  $\Phi_1(z)$ , dashed line; relative upward flux  $\Phi_2(z)$ , dash-dot line; and relative net flux  $\Phi_n(z)$ , solid line for light at 675 nm wavelength inside a horizontal dorsiventral leaf with light incident on the palisade parenchyma (#1 and #2) and light incident on the spongy mesophyll (#3 and #4), for illumination zenith angles of 25° (#1 and #3) and 65° (#2 and #4). Gray lines (filled circles) indicate the cumulative chlorophyll concentration, expressed in  $\mu\text{g cm}^{-2}$ . Symbols are UE upper epidermis, PP palisade parenchyma, SM spongy mesophyll, and LE lower epidermis. (Panels 1 and 2 were modified from Ustin et al. (2001) with permission from Wiley and Sons. Panels 3 and 4 were not previously published)

the stomatal (or substomatal) cavity. The stomata open and close, regulated by turgor pressure, to allow gases, including water vapor, C dioxide, and oxygen, to exchange between the outside air and the stomatal cavity. Because the anatomical structures of species are different across the interior of the leaf, their biochemistry is also specialized, causing the asymmetric distributions of reflectance and absorption patterns as light passes through the leaf, shown in Fig. 14.4, for photosynthetic light at two solar zenith angles entering from the lower side of the leaf.

Xerophytes and hydrophytes illustrate the extremes of leaf adaptations for cuticle characteristics. Aquatic species that float on the surface like water hyacinth (*Eichhornia crassipes*) and water lily (*Nymphaea* sp.) have stomata on the upper, adaxial side that is open to the atmosphere. Submerged aquatic species, like Brazilian waterweed (*Egeria densa*), hydrilla (*Hydrilla verticillata*), and Eurasian watermilfoil (*Myriophyllum spicatum*), lack stomata or they are nonfunctional, and their cuticle is thin and reduced to allow direct gas exchange with the water. These species typically have other morphological traits that support adaptation to the aquatic habitat, including very small leaves. In contrast, xerophytes like semiarid grasses, e.g., the beach grass *Ammophila breviligulata*, and conifers or succulent species like agaves and cacti, have stomata in deep pits that reduce transpiration by retaining high vapor pressure in the cavity. In addition, other traits typically present in xerophytes include thick cuticles, pubescence, and a reduced stomatal complex. Leaf traits such as these tend to be clustered, representing a suite of adaptive traits; thus, to identify a taxon, we expect several traits to be present in particular configurations; thus, potential identification is enhanced by patterns of traits (see Serbin and Townsend, Chap. 3; Morsdorf et al., Chap. 4; Bolch et al., Chap. 12).

### 14.7.1 Surface Characteristics of Epidermal Cells

Epidermal cells can be coated with smooth wax, which enhances specular scattering off the surface of leaves. This type of surface scattering occurs when the leaf is oriented to cause forward scattering of incoming beam. Light specularly scattered from a leaf surface has the same wavelength composition and intensity as the incoming beam, so it does not provide any information about the interior of the leaf. Smooth, waxy leaves having shiny, glabrous surfaces are often found in young leaves of broadleaf shrubs, trees, or herbaceous understory species. In woody plants, this is generally a mechanism to avoid absorbing excess photosynthetically active radiation under high light conditions. Species that have this trait include members of *Cinnamomum* in the laurel family (e.g., *Cinnamomum camphora* and *C. parthenoxylon*) and *Magnolia grandiflora*, which are found in warm subtropical habitats, often in the understory.

The waxy cuticle or outer layer of the epidermis produces a 3-D structure of waxes and cutin of variable thickness and cell types that create a diverse range of textured surfaces and colors. Leaf traits like thick cuticles are common to a wide range of plants such as columnar cacti (e.g., *Pilosocereus leucocephalus*) and

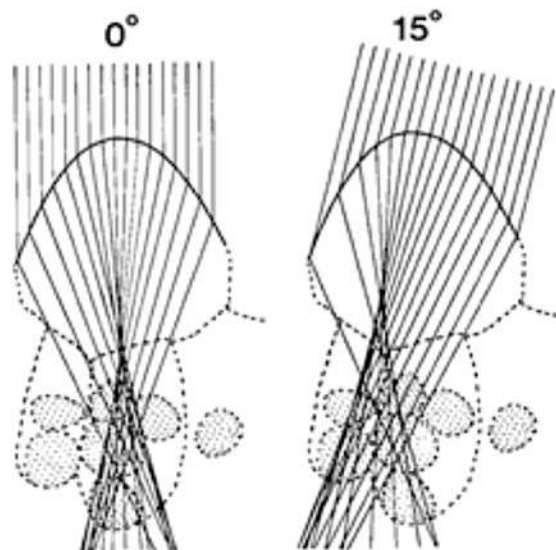
conifer species like the blue Colorado spruce, *Picea pungens*. These plants are often found in high light or drought-stressed environments, or at high elevations, where they may be exposed to high UV radiation.

### 14.7.2 Epidermal Cell Shape and Function

The outer (adaxial) surfaces of epidermal cells form convex shapes. This shape has been shown to focus light into the palisade parenchyma cells (Fig. 14.5), increasing light capture for photosynthesis (Haberlandt 1914; Martin et al. 1989; Bone et al. 1989; Poulson and Vogelmann 1990). Light focusing is a widespread property in seed plants and is common in prairies, deserts, and deciduous forests (Vogelmann et al. 1996b), especially in plants from understory species (e.g., *Medicago sativa*, *Impatiens* spp.) and other species growing in low light conditions. Light focusing increases the photon density (up to 10 $\times$ ) inside the palisade parenchyma cells, and given the mobility of chloroplasts in the palisade parenchyma cells, they assist in optimizing the light environment within the leaf (Poulson and Vogelmann 1990).

The shape of the epidermal cells affects the focal length. By changing the turgor pressure in the epidermal cells, a plant can decrease focal length to increase the absorbing area in shaded habitats or increase it to penetrate deeper into the palisade parenchyma. This ability increases the probability of light absorption and thus is beneficial for leaves in low light environments (Vogelmann et al. 1996a, b; Smith et al. 1997).

**Fig. 14.5** Refraction of rays at two different solar zenith angles of 0° (perpendicular to surface) and 15° off vertical in epidermal cells of *Anthurium warocqueanum*. Light is focused on the palisade parenchyma below the single layer of epidermal cells. (Reproduced from Poulson et al. (1989) with permission from the Optical Society of America)



### 14.7.3 *Epidermal Cell Index of Refraction*

As light passes into and through the epidermal cell walls and into mesophyll cells, it is scattered in new directions, based on differences in the velocity with which different wavelengths move between the cell solution and the air spaces. The refractive index determines how much the light is bent between different media, as described by the Snell–Descartes' law, which says that the biochemical constituents of the leaf determine the speed of light passing through it relative to its speed in a vacuum. The effective refractive index of leaves varies with the biochemical composition of different species. It also varies with the wavelength of light, as seen when white light is split into its individual colors by a prism. Each wavelength is bent at a different angle, from  $40^\circ$  to  $42^\circ$ , causing separation of the colors. The angles of incidence and refraction at the interfaces between the mesophyll and the cell walls influence the leaf's optical properties by affecting the probability that light is multiply scattered through the cell interior, escapes directly out of the leaf after the first interaction with a surface, or is absorbed.

The refractive index is a complex number in which the real part is the refractive index and the imaginary part is related to the extinction coefficient (also called the mass absorption coefficient), which accounts for light attenuation when photons pass through a medium. These values change across the optical spectrum, and it has not been easy to determine the refractive index for most plant compounds; only pure liquid water has been fully characterized. Thus, in most cases, the refractive index and extinction coefficient cannot be measured directly and must be estimated from measurements of properties that depend on them, such as reflectance and transmittance. Since the 1950s, a long list of investigators have improved knowledge of the real and imaginary parts of the refractive index for water in different regions of the electromagnetic spectrum (e.g., Segelstein 1981; Hale and Querry 1973; Wieliczka et al. 1989) as shown in Fig. 14.6. Because these coefficients change with the phase of water (vapor, liquid, or solid) and its temperature, the phase needs to be specified. Curcio and Petty (1951) were among the first to accurately measure absorption coefficients for liquid water between 700 nm and 2500 nm at 20 °C; they identified absorptions at 760, 970, 1190, 1450, and 1940 nm. Except for the water absorption feature at 760 nm, the liquid water bands at 970 and 1190 nm are readily observed in canopy and leaf spectra. In the laboratory, we observe the much stronger liquid water absorptions at 1450 and 1940 nm; however, in satellite and airborne imagery, these wavelengths are usually saturated with atmospheric water vapor, which has significantly higher concentration over the full atmospheric column than does liquid water in the leaf. As with other molecular absorptions (pigments, liquid water, dry biomass, etc.), as the amount of water vapor increases, the wavelength bands on the shoulders of the absorption maximum also absorb energy, and the feature expands over more wavelengths. Generally, acquisition of airborne imagery is avoided under rainfall or high water vapor conditions because clouds obscure the ground in optical imagery; hence, archives have little data acquired under high liquid water atmospheric conditions.

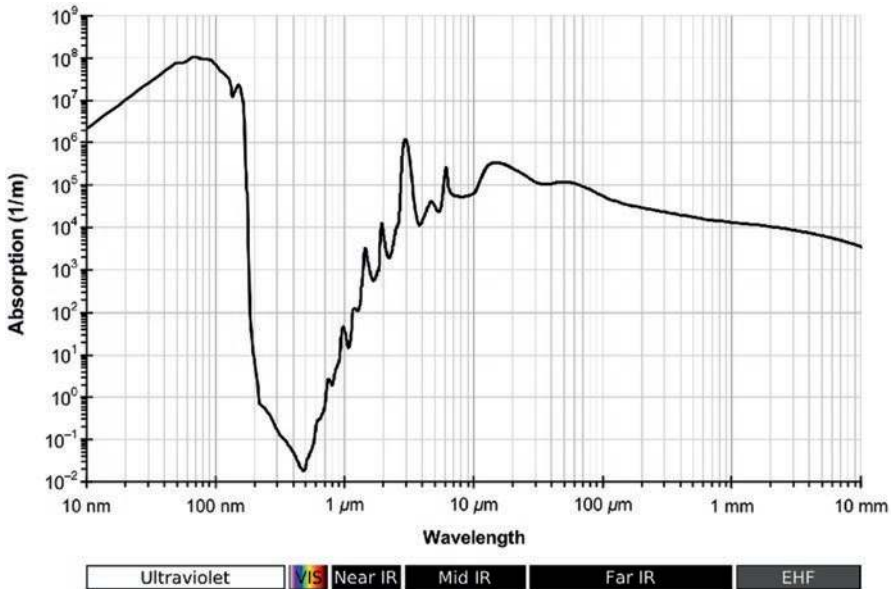


**Fig. 14.6** Liquid water absorption spectrum showing the imaginary part of the refractive index, the absorption coefficient. Created 1 July 2008, compiled by Kebes ([https://commons.wikimedia.org/wiki/File:Absorption\\_spectrum\\_of\\_liquid\\_water.png](https://commons.wikimedia.org/wiki/File:Absorption_spectrum_of_liquid_water.png)). Accessed 30 Nov 2018) at English Wikipedia CC by SA 3.0 (<http://creativecommons.org/licenses/by-sa/3.0>). Based on Segelstein (1981), Hale and Querry (1973), and Wieliczka et al. (1989); other references at <http://omlc.ogi.edu/spectra/water/abs/index.html>

## 14.8 The Mesophyll

The leaf mesophyll includes all cells between the two epidermal layers and consists of one or more types of ground parenchyma, depending on the cellular specialization. Because these tissues are arranged differently in dicots, monocots, and conifers, spectral responses frequently differ among the three groups. Other taxa, including mosses and ferns, also have different characteristic foliar anatomy and biochemistry that allows them to be distinguished from higher plants by their spectral characteristics (Vogelmann and Moss 1993; Bubier et al. 2007; Van Gaalen et al. 2007). Monocots and conifers generally have one type of ground tissue, called chlorenchyma, which are chloroplast-containing parenchyma cells, while dicot leaves typically have two types of parenchyma cells: elongated densely packed cells that are oriented perpendicular to the upper leaf surface and termed palisade parenchyma and irregular-shaped cells with a high proportion of air spaces in the tissue, called spongy mesophyll (Fig. 14.3). The mesophyll tissue also includes the vascular tissue that transports water and nutrients into the leaf and carbohydrates out of the leaf. These cells are generally within a larger tissue termed the vascular bundle, which includes xylem and phloem cells that conduct fluids and fiber cells and tracheids that provide structural support for the leaf and the conducting tissue. The conducting cells are connected throughout the leaf in a network of veins.



### 14.8.1 *Mesophyll Index of Refraction*

The refractive indices of cell walls in the visible wavelengths have been empirically estimated to be 1.4 (Knippling 1970), 1.425 (Gausman 1974), and 1.415 in living cells and 1.53 in dried cell walls (Woolley 1975). It is very difficult to characterize the refractive index for pigments, cellulose, cell walls, proteins, etc. given our inability to measure them in situ. One reason the refractive index is known for so few plant biochemicals is that in their functional state, these cell constituents are bound to membranes in complexes with proteins and other molecules, so when they are isolated, their 3-D structure has been lost along with their bond structures and other molecular interactions. The function of proteins, pigments, enzymes, (including ribulase-1,5-bisphosphate carboxylase, RUBP-Case, RuBisCO), and amino acids (all of which contain N) depends on their structure, and empirical methods have not worked well to obtain their absorption coefficients in vivo, so they cannot be accurately predicted in radiative transfer models. It has long been known that N is generally allocated proportional to optimal photosynthesis (Field and Mooney 1986). More than half of all leaf N is allocated to photosynthetic proteins (Makino and Osmond 1991; Hikosaka and Terashima 1996). Because N forms many types of bonds, it has been necessary to estimate the total concentration of foliar N from training data in empirical models, based on either photosynthesis models or statistical models like partial least squares and other self-learning methods (see Serbin and Townsend, Chap. 3). In recent years, statistical methods have become the preferred approach to estimate leaf N concentration. These can be accurately applied as long as the new data have the same statistical structure and ranges as the original test data. The total concentration of foliar N is often predicted directly from empirical models using methods like partial least squares regression (Smith et al. 2002; Ollinger and Smith 2005; Singh et al. 2015) or, more recently, by self-learning methods, such as wavelets, used by Cheng et al. (2014) to estimate leaf mass area (dry weight  $\cdot$  area<sup>-1</sup>). These methods can easily be overfitted, so care is needed to produce a realistic result (Féret et al. 2011). Nonetheless, these models can be accurate for the vegetation types and concentrations they are trained against, and they are being used to estimate functional properties and biological diversity (Asner et al. 2014a, b; Asner and Martin 2016; Féret et al. 2014a, b).

### 14.8.2 *Molecular Absorption Processes*

For a wavelength of light to be absorbed, the amount of energy in a photon must equal the specific energy difference between the resting (ground) state of the electron ( $S_0$ ) and its excited state in an allowable unoccupied higher energy level (Fig. 14.7). It is the separation of water into an  $H^+$  and an  $OH^-$  ion that provides the electron that is transferred through the electron transport chain in photosynthesis. The magnesium ion in the tetrapyrrolic ring of the chlorophyll molecule helps initially stabilize the charged state long enough to transfer it to a phaeophytin in the

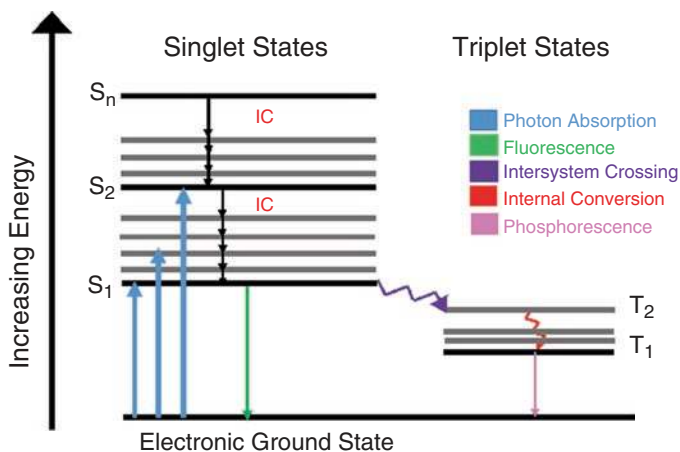


**Fig. 14.7** Jablonski diagram showing energy levels for a chlorophyll  $\alpha$  molecule excited by light absorption. The excited electron states  $S_1$  and  $S_2$  are excited singlet states at wavelengths effective for electron transfer for photosystem II. Gray lines represent spin multiplicity states (usually vibrational or rotational) within the main electronic energy states (bold lines). The Soret bands ( $S_n$ ) excite electrons for photosystem I at the shorter wavelength excitation peak for chlorophyll  $\beta$ , overlapping with chlorophyll  $\alpha$  and facilitating energy transfer. As electrons return to the ground state, energy can undergo internal conversion (IC) to the  $S_2$  or  $S_1$  states or be released by emission as fluorescence. Under slow energy transfer pathway (termed *intersystem crossing*), the  $T_1$  and  $T_2$  excited triplet states can release energy as phosphorescence. Derived from multiple sources

excited P680\* complex and from there to plastoquinol, the first step in the electron transport chain. The energy is passed to the cytochrome b6f complex and to plastocyanin in the path to the reaction center at photosystem I (PS I) and, from there, ultimately to NADP<sup>+</sup> and ADP. In their reduced state, they provide energy to reduce CO<sub>2</sub> to a 3-C sugar in the Calvin cycle. The enzyme catalyzing the CO<sub>2</sub> reduction reaction is RuBisCO, which is the most abundant protein on Earth (Ellis 1979; Cooper 2000; Raven 2013).

### 14.8.3 Leaf Biochemistry and Energy Absorption in the Solar Spectrum

The chemistry of plant species may be highly variable in terms of secondary compounds, but essential physiological functions are similar. Because seed plants share a common ancestry and face common requirements to survive, younger species retain structures based on their genetic heritage to capture and use sunlight. For a species to survive in a particular environment, the suite of leaf traits must be consistent with long-term patterns of environmental resources, and investments in plant tissues and biochemical composition are determined by metabolic activities, as illustrated by correlations among environmental conditions, leaf chemistry, and

physiological functions and as shown in the TRY leaf trait database (Kattge et al. 2011). Studies show loose stoichiometric relationships between different biochemical elements such as C, N, and phosphorus and growth rates and biomass accumulation. Although the relationships vary with conditions and species, typically, C shows relationships with  $X$  (biochemical) where the  $C/X$  ratio increases under nutrient-limited growth, increasing light intensity, and partial pressure of  $CO_2$  and as a function the species (Sterner et al. 2002).

We expect that to maintain high levels of productivity, leaf chemistry associated with light harvesting and reduction of  $CO_2$  must be correlated, such as chlorophyll a and b and N concentrations, and correlations with other nutrients and water content are all available at appropriate levels for leaves to achieve high productivity. This is formulated in concepts of plant functional morphology (Tilman 1985; Chapin et al. 1993), which emphasize trade-offs in allocation of resources. For example, allocation should shift to shoots under low light and high nutrient conditions and to roots under high light and low nutrient conditions. Ackerly (1999) show that under conditions of high fertility, high rates of growth produce self-shading in older leaves that are lower in the canopy. This limits available light and results in declining rates of assimilation for older leaves. Field (1983) reported that older leaves had reduced N concentrations and photosynthetic potential. Other studies have shown that canopies with steep light gradients exhibit greater declines in photosynthetic capacity than those with small gradients (Mooney et al. 1981). These relationships result in high nutrient environments being favorable to deciduous trees with high growth rates, low C/N ratios, and high rates of leaf and root turnover. Under low nutrient conditions and high light environments, plants exhibit slower growth rates and higher root/shoot ratios. Competition would favor slow growth and low stature species with high nutrient retention and higher C/N ratios. The ratio of leaf dry mass per unit leaf area seems to be highly correlated with growth potential, and species with low mass per unit area have high potential growth rates and high rates of C uptake, while species with high leaf mass area have low growth potential but are generally more stress tolerant (Wright et al. 2004). Of course, all species fall somewhere on this range, but annuals are expected to be at the higher growth end, deciduous woody species are expected to have higher values than evergreen species, and those with thick leathery evergreen leaves are expected to score among the lowest values.

Today, with the development of imaging spectrometry, there is active research aimed at understanding the significance of different assemblages of leaf traits (and their associated chemistry), the roles they play in adaptation for specific habitats, and how they can be detected from spectral patterns measured with optical sensors (Féret and Asner 2014a; Asner et al. 2014b, 2015; Serbin et al. 2015; Singh et al. 2015; Couture et al. 2016). The concept of detecting plant traits has jumped from RS and ecological research to rapid testing of crop breeding of new genotypes through high-throughput phenotyping (Araus and Cairns 2014; Li et al. 2014). The current procedures are derived from precision farming but involve high spatial resolution (using differential GPS) multiple RS inputs, commonly including lidar, thermal infrared, imaging spectrometers, fluorescence imagers, and multiband imagery

to rapidly characterize phenotypic variability in relation to desired crop attributes like resistance to disease or other stressors while retaining high growth potential (Bai et al. 2016; Tanager et al. 2017). Such combined methods would provide better resolution of biodiversity in natural systems than use of a single instrument data type.

#### 14.8.4 Photosynthetic Pigments

Light absorption by pigments in the chloroplast produces a unique absorption pattern in the visible spectrum, with higher absorption in the blue and red wavelengths than in the green wavelengths. All higher plants have chlorophyll a and b in their photosynthetic tissues. Absorption features in the visible to NIR part of the spectrum are predominantly caused by excitation of electrons in a process called electronic transitions, in contrast with bending and stretching of molecules in the infrared bands.

Chlorophyll b is nearly identical to chlorophyll a (Fig. 14.8) except that an aldehyde replaces the methyl on the chlorin ring, opposite the phytol tail. This difference affects which wavelengths are absorbed; chlorophyll b has peak absorptions at 450 nm and 642 nm (blue–green), whereas chlorophyll a absorbs primarily at 590–720 nm (orange–red). Because its absorption peaks in these bands are at longer (455 vs. 429 nm) and shorter (642 vs. 659 nm) wavelengths than chlorophyll a, chlorophyll b can transfer its excited electron to the reaction center of chlorophyll a (P680). The chemical composition and structure of accessory pigments increase the range of wavelengths that can capture energy for photosynthesis. While all seed plants all share chlorophyll a and b, they differ in the concentrations of the suite of carotenoids found in chloroplasts. The composition of chlorophylls, carotenoids, and anthocyanin pigments in different species provide a basis for using remote sensing data to differentiate species and perhaps phylogenetic relationships among related species and could contribute to biodiversity monitoring.

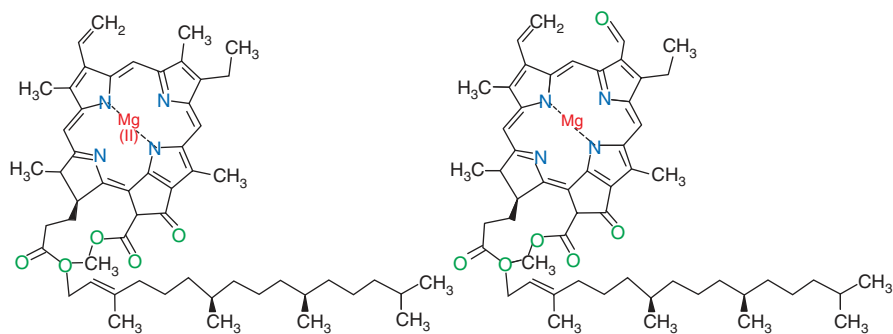


**Fig. 14.8** Chlorophyll  $\alpha$  and  $\beta$  molecules. (Modified from ChemSpider <http://www.chemspider.com> and reproduced with permission of the Royal Society of Chemistry)

The optical properties of pigments have been characterized after extraction from chloroplasts (Fig. 14.9). However, these properties are not the same as they are in the intact chloroplast and leaf because extraction alters the chemical environment and destroys the bond structure in their functional state of the pigment–protein complexes. The light-harvesting pigment–protein complexes are associated with other molecules in the chloroplast that affect their three-dimensional configuration and, hence, their absorption patterns. The polarity and water content of the solvents used to extract chlorophylls also shift their peak absorption wavelengths (Lichtenthaler 1987, Fig. 14.9).

One alternative to using extractive chemistry to determine the absorption coefficients of pigments is to use inversion of radiative transfer models. The PROSPECT family of models are the most widely used leaf optical properties models; the recent

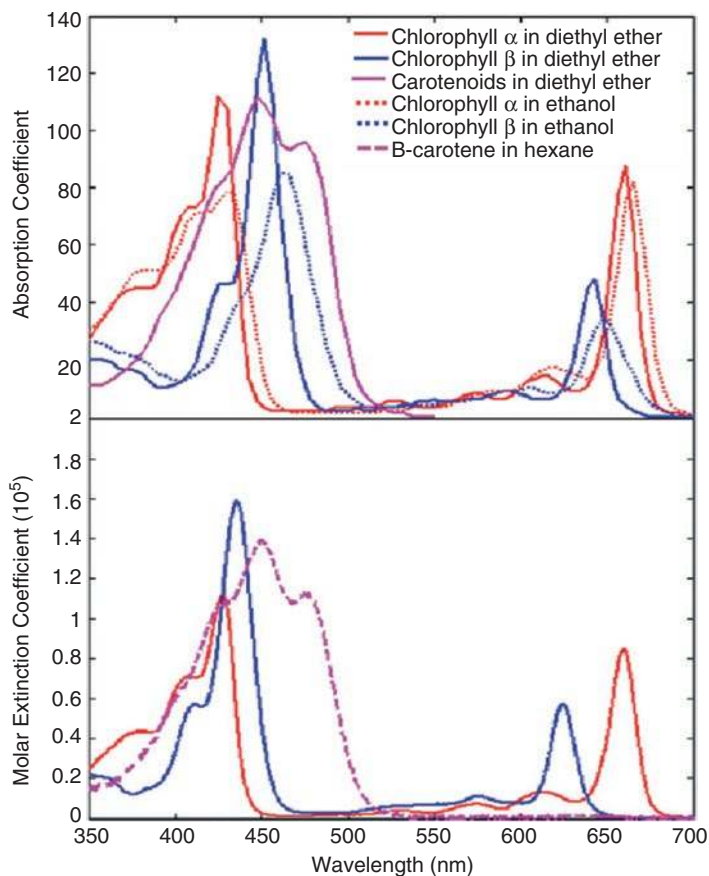


**Fig. 14.9** The spectral shape of chlorophylls and carotenoids extracted in different solvents. (Data redrawn from Lichtenthaler (1987) and Du et al. (1998); reproduced from Ustin et al. (2009), with permission from Elsevier)

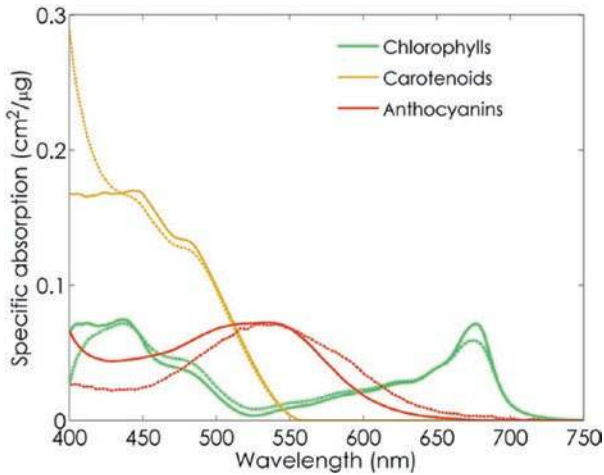


**Fig. 14.10** Specific absorption coefficients for total chlorophyll and carotenoids derived from PROSPECT-D (Féret et al. 2017) are shown in solid lines. Dashed lines are the specific absorption coefficients from PROSPECT 5 (Féret et al. 2008). The specific absorption coefficients of anthocyanins were measured by Peters and Nobel (2014). (From Féret et al. (2017), reprinted with permission from Elsevier)

version, PROSPECT-D (Féret et al. 2017), used a large database of leaf spectra and chemistry to predict the in-situ absorption coefficients for chlorophyll, carotenoid, and anthocyanin pigments. Figure 14.10 shows that the modeled absorption coefficients of in-situ pigments are broadened and compressed relative to the extracted pigments.

### 14.8.5 Accessory Pigments

In the light-harvesting complex, chlorophyll b and carotenoids enhance capture of photons and pass them to the reaction centers of the two photosystems. Carotenoids are produced in plastids in all plant organs (Beisel et al. 2010); however, those in leaf chloroplasts are critical to photosynthetic functioning. Carotenoid species are under constant synthesis and degradation (Beisel et al. 2010), although total concentrations remain approximately equal to the concentration of chlorophyll *a*. Carotenoid molecules are composed of 40-C polyene backbone structures with different side chains. Common chloroplast carotenes include  $\alpha$ -carotene and  $\beta$ -carotene, which have oxygen-free structures and are considered primary carotenoids due to their photosynthetic function. Lutein and other forms of carotenoids that have oxygen in their structure are known as xanthophyll pigments; they help regulate energy in the chloroplast (Lichtenthaler 1987). Concentrations of specific carotenoids and pool size vary between species (Thayer and Björkman 1990) and with environmental



conditions such as sun vs. shade, cold temperature, and others (Thayer and Björkman 1990, Demmig-Adams and Adams 1992, Hannoufa and Houssain 2012). For example, some species with shade-grown leaves may have high concentrations of  $\alpha$ -carotene, and some with sun-grown leaves have only trace concentrations (Thayer and Björkman 1990). Comparing among species with shade-grown leaves, concentrations of lutein or neoxanthin can vary as much as factors of two (Thayer and Björkman 1990). Such differences in concentrations of specific carotenoids and/or their pool sizes provide potential for use in identifying biodiversity patterns if remote sensing instruments and analytics have power to resolve some of these differences.

### 14.8.6 Xanthophyll Pigments

Oxygen-containing carotenoids contribute to regulation of photosynthetic functioning. For example, a reversible bond changes between violaxanthin and zeaxanthin as light environments change from low light to high light conditions, causing a small increase in reflectance around 530 nm that protects the photosynthetic reaction center from the additional light. Gamon et al. (1992) provided the first experimental evidence that this signal could be measured with spectrometers. The photochemical reflectance index (PRI) by Gamon et al. (1992) has had extensive use and is assumed to follow short-term (minutes to hours) xanthophyll cycle changes; over longer periods, the PRI more likely represents changes in chlorophyll/carotenoid ratios (Gamon et al. 2015).

#### 14.8.6.1 Apparent Concentration vs. Actual Concentration

In some cases, the apparent concentration of a chemical is overestimated or underestimated due to the probability of light interacting with weakly or strongly absorbing chemicals in nonhomogeneous media. An *in vivo* phenomenon termed the *detour effect* increases the probability of absorption for nonhomogeneous distributions of weakly absorbing molecules (Fukshansky et al. 1993; Terashima et al. 2009). This effect lengthens the optical path length within the leaf and increases photon scattering, enhancing the potential for a weakly absorbing molecule to interact with the photon (Terashima et al. 2009). A different phenomenon termed the *sieve effect* has, generally speaking, an opposite effect. The sieve effect decreases the expected absorption by concentrating strongly absorbing molecules (pigments, water, and other compounds) in a small area of the cell volume (e.g., in organelles). Consequently, the molecules have more limited opportunities to interact with a photon and be absorbed. It effectively reduces the path length, and its effect is most noticeable at wavelengths where light is strongly absorbed [e.g., chlorophyll pigments in the blue and red wavelengths (Evans et al. 2004) or water in the SWIR (Baranoski and Eng 2007)]. Terashima et al. (2009) show that for weakly absorbed light such as in green wavelengths, the loss of absorption due to the sieve effect is

minimal, while the gain in absorption by the detour effect is large. The detour effect can increase absorption at 550 nm sufficient to rival absorption in blue and red bands for photosynthesis. Such interactions make quantifying the concentrations of specific compounds and correctly attributing their impact on physiological processes subject to potentially significant errors. Despite difficulties in separating the effect of each pigment in the leaf, the *in vivo* spectral shapes of different species are fairly conservative within related taxa and are often distinctive of the taxonomic group over much of the wavelength region between 450 nm and 700 nm; these patterns have been used to identify genera, species, and even phenotypes (Asner and Martin 2016; Junker and Ensminger 2016).

### ***14.8.7 Non-photosynthetic Pigments***

Anthocyanins are a diverse group (more than 540 pigments identified in nature; Anderson and Francis 2004) of colored, water-soluble flavonoids found in the vacuoles of many seed plants (Hrazdina et al. 1978). Pigment colors range from blue to red, depending on pH. Anthocyanins have been associated with many benefits to plants (Lee and Gould 2002). They attract pollinators and animals that disperse seeds and fruits, protect plants growing at high elevations from UV light, and protect against cold (Chalker-Scott 1999; Lee 2000). Anthocyanins are common in understory plants (Lee 2002). The protective mechanism of anthocyanins in leaves develops during early stages of leaf expansion (e.g., young leaves in Fig. 14.2) before leaves are photosynthetically functional in some species (Landi et al. 2015). Lee and Collins (2001) showed within-family phylogenetic relationships of anthocyanins for 399 woody tropical taxa. Other flavonoids also contribute to physiological regulation, providing chemical signals to other parts of the plant or to other plants, or promoting or inhibiting interactions with other organisms. Because of their strong absorption in the red wavelengths, anthocyanins can be confused with chlorophylls, resulting in overestimation of photosynthetic capacity. Gitelson et al. (Gitelson 2012) developed semi-analytic three-band models to separately estimate the concentrations of chlorophylls, carotenoids, and anthocyanin foliar pigments. In collaboration with Gitelson, Féret et al. (2017) updated most recent PROSPECT-D model (Féret et al. 2017) fusing a linear relationship among six independent data sets between predicted and measured anthocyanin. Féret et al. (2017) improved the specific absorption coefficients for chlorophylls, carotenoids, and anthocyanins as shown in Fig. 14.10.

### ***14.8.8 Brown Pigments***

When pigments and their protein complexes degrade, they form colored chemical residues. These are poorly described but constitute the “brown” pigments or colored pigment residues in the leaf when it senesces and dies. These result from oxidation

and polymerization of cell constituents. Without pigment residues, cellulose and other cell wall materials would be a nearly colorless white. Regardless of plant species, there is a general trajectory of color change over time. Brown pigment residues produce the shades of light tan colors found in recently dead leaves. The residues further degrade and become darker over winter. Eventually, they become dark brown and chemically and spectrally indistinguishable from humus (Ziechmann 1964). The visible near-infrared shape of the absorption spectrum for recently dead plant residues is generally monotonic, lowest at 400 nm and increasing in a polynomial curve to about 900 nm.

## 14.9 Leaf Water Content

The optical properties of water are better known than those of any other plant biochemical. In recent years, there have been several attempts to improve the absorption coefficients for liquid water; but since there have been no major changes, we assume this property is mostly resolved for liquid water.

The optical properties of water are known with much greater precision than are those of pigments or other molecules. Water absorptions are due to vibration of the molecules, with a vibrational frequency that approximates simple harmonic motion when excited by absorbing a quantum of energy. Because hydrogen atoms are small, vibrations have large amplitude. Water vapor has three fundamental vibrational modes with the dipole moments changing in the direction of the vibration (Fig. 14.11). The first mode for liquid water at 25 °C is symmetric stretching; in this case, both hydrogen ions vibrate simultaneously, which is at mode  $\nu_1$  with a 3050 nm absorption feature. The second vibrational mode is bending the covalent bonds, which occurs when the two hydrogen atoms vibrate by moving toward and away from each other. This bending mode is at mode  $\nu_2$  and it causes a strong absorption at 6080 nm. The third mode is asymmetric stretching that results from one hydrogen ion being attracted toward the oxygen while the other moves away. The absorption wavelength for this  $\nu_3$  mode is 2870 nm. Vibrational modes for liquid water at shorter wavelengths (401–1900 nm) are combination modes. Vibrational modes are restricted in liquid water and ice by hydrogen bonds. *Libration* describes the back-and-forth rotation of the hydrogen ions in liquid water when its motion is restricted.

The infrared spectrum of water results from vibrational overtones and combinations with librations. Palmer and Williams (1974) conducted a detailed study, including verification of prior authors (e.g., Hale and Query 1973) and reported 94 optical constants between the UV and the NIR. They report liquid water values related to those in Table 14.1 for measurements taken at 27 °C to be 769, 847, 973, 980, 1205, 1443, 1786, and 1927 nm. Kou et al. (1993) established absorption coefficients for ice between 1440 and 2500 nm, showing that these peaks are at longer wavelengths than those of liquid water when measured at warmer temperatures. Wieliczka et al. (1989) developed an improved measuring device, measured the real part of the refractive index, and used it with Kramers–Kronig methods to compute

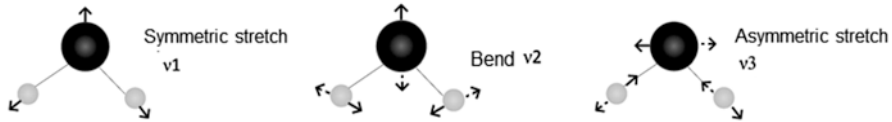


**Fig. 14.11** The vibration modes in liquid water from overtone and combined overtone bands in the near-infrared (NIR)

**Table 14.1** Vibrational–rotational transitions for water vapor, liquid water (near 100 °C), and ice

Gas	Liquid (near 100 °C)	Liquid (near 0 °C)	Ice	Vibrational assignment
Wavelength (nm)	Wavelength (nm)	Wavelength (nm)	Wavelength (nm)	
723	740	770	800	$3 \nu_1 + \nu_3$
823	840	847	909	$2 \nu_1 + \nu_2 + \nu_3$
1025	967	979	942	$2 \nu_1 + \nu_3$
1250	1160	1200	1135	$\nu_1 + \nu_2 + \nu_3$
1492	1425	1453	1380	$\nu_1 + \nu_3$
1780	1786	1780	–	$\nu_2 + \nu_3 + \nu_L$
1988	1916	1938	1875	$\nu_2 + \nu_3$

From Workman and Weyer (2008), modified with permission from Taylor and Francis

$\nu_1$  is the symmetric stretch,  $\nu_2$  is the bending mode,  $\nu_3$  is the asymmetric stretch, and  $\nu_L$  is the undefined “intermolecular mode”

the imaginary part. Buiteveld et al. (1994) conducted detailed measurements of pure water over temperatures from 25 to 40.5 °C and improved absorption coefficients over the range of 300–800 nm. Féret et al. (2017) combined these in developing the PROSPECT-D model and tested the inversion on leaf data from six data sets with a total of 521 leaves. From this, they derived the absorption coefficients for pure water, shown in Fig. 14.12 covering the 400–2500 nm region.

The atmosphere is nearly always saturated with water vapor at 1450 nm and 1940 nm (Fig. 14.13). Published imaging spectrometer data are typically shown with these wavelengths deleted since only in the driest deserts is there a possibility of observing the ground surface from airborne or satellite sensors (see also Segelstein’s (1981) absorption coefficients, Fig. 14.6). A series of increasingly strong water vapor absorptions are observed from the visible region, around 512 nm to the SWIR at ~2500 nm. Because the absorption maximum of each phase of water at 940–1020 nm is offset by 30–40 nm, it is possible to identify and quantify whether water is present in vapor, liquid, or solid phases in imaging spectroscopy data having bandwidths of 5–10 nm. The second absorption region for detecting the three phases of water is located at 1100–1300 nm. Absorptions are too strong beyond

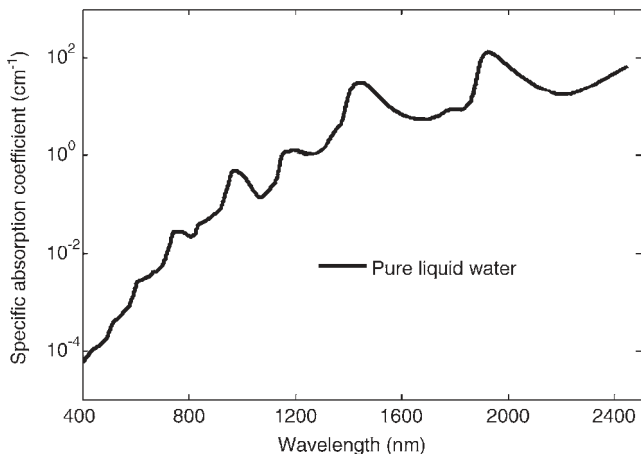


**Fig. 14.12** Féret et al. (2008) developed a new absorption coefficient for water for the PROSPECT 4 and 5 model built by combining data from Buiteveld et al. (1994) at 400–800 nm, Kou et al. (1993) at 800–1232 nm, and Wieliczka et al. (1989) at 1232–2500 nm. The model was evaluated by testing on six independent leaf data sets. (Reproduced by permission from Elsevier)

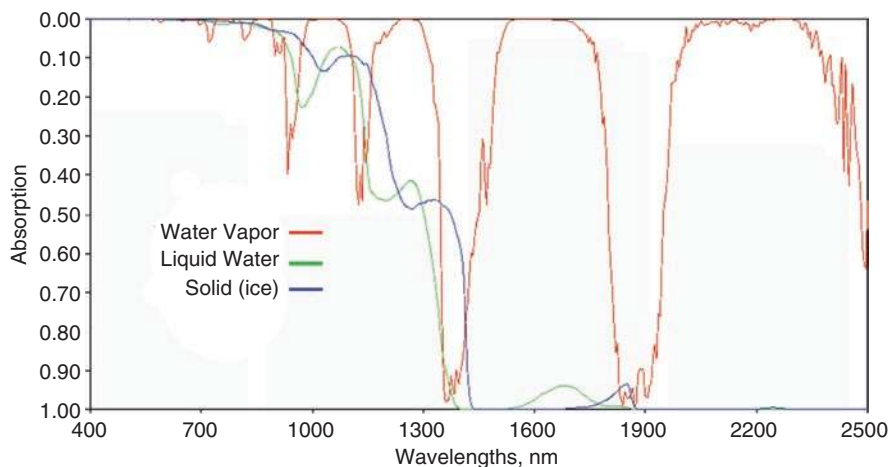


**Fig. 14.13** The absorption spectrum at 400–2500 nm for vapor, liquid, and ice phases of water. For each absorption feature, water vapor (shown in red) is at the shortest wavelengths, and ice (shown in blue) is at the longest wavelengths. (Figure from Robert O. Green, NASA Jet Propulsion Laboratory)

these wavelengths to easily measure them in the optical region. Airborne imaging spectrometer data use one or both of the two wavelength regions (940–1020 nm and 1100–1300 nm) for calibrating an RT model for absorptions and scattering in the atmosphere to fit to the measured spectrum. The water vapor, liquid water, and ice concentrations are then estimated from the best fit of the RT model.

## 14.10 Cell Wall Constituents

The organic compounds that make up the cell wall comprise about 75–90% of the dry weight of the leaf. They vary with the location in the leaf, by phenology (season), with environmental stressors, and by species. They also vary depending on whether the walls are primary or secondary structures or part of the vascular bundles. Common constituents include cellulose, hemicellulose, lignin, proteins, and pectins. They are large molecules of variable molecular composition; their –OH units form extensive hydrogen bonds that link the molecules together, providing both flexibility and strength. They form solid structures and are mostly insoluble. This makes them poor candidates for spectroscopy, so they are generally measured with other techniques.

Cellulose is the most abundant organic polymer on Earth (Klemm et al. 2005). It is a polysaccharide forming a straight chain of many to thousands linked D-glucose units (Fig. 14.14a) with a nonreducing end (shown on left) linked to repeating glucose units by oxygen and ending with a reducing oxygen ion. The –OH groups form hydrogen bonds across chains, holding them together and providing structure. Species can be identified based on the relative abundance of these molecules.

Hemicellulose refers to any of several heteropolymers that form the matrix polysaccharides in most plant cell walls (Fig. 14.14b). Hemicellulose monomers include hexoses and fructoses such as xyloglucans, xylans, and glucans. Figure 14.15 illustrates some differences in hemicellulose subunit structures. Their chemical composition is similar to that of cellulose, so they are spectrally similar and are not generally separately identified in leaf spectra. The structure of these molecules, however, varies between species, suggesting that they could contribute to identifying biodiversity from RS data and possibly different species or related species.

Lignins are a widely distributed class of complex amorphous organic, branched, and cross-linked polymers (Fig. 14.14c) of the approximate composition  $C_{31}H_{34}O_{11}$ . They form the structural materials of cell walls and other support tissues in leaves, such as the walls of tracheids in the vascular system. Lignin is unusually heterogeneous in composition and lacks a defined primary molecular structure. Figure 14.14c illustrates the cross-linked phenol units that make it very slow to decompose. Eventually, the recalcitrant residues become a major fraction of the soil humus. Humus is important in the global C cycle for sequestering soil C and nutrients and retaining soil moisture. Lignins interact with soil organic matter and N turnover rates, and this affects lignin stabilization (Thevenot et al. 2010), so they are important in biogeochemical cycling. The variety of lignin molecules found in different plant species makes quantification difficult, but some forms are known to occur in specific plant clades, providing a basis for estimating diversity between lower vascular plants, conifers and angiosperms (Weng and Chapple 2010) (Fig. 14.15).

Although fundamental frequencies are known for C–H, C=O, C–N, O–H, and N–H bonds, dried and powdered leaf materials have overlapping spectral properties of various cell wall molecules, proteins, enzymes, amino acids, sugars, starches, waxes, and other biomolecules that make it difficult to isolate specific molecules



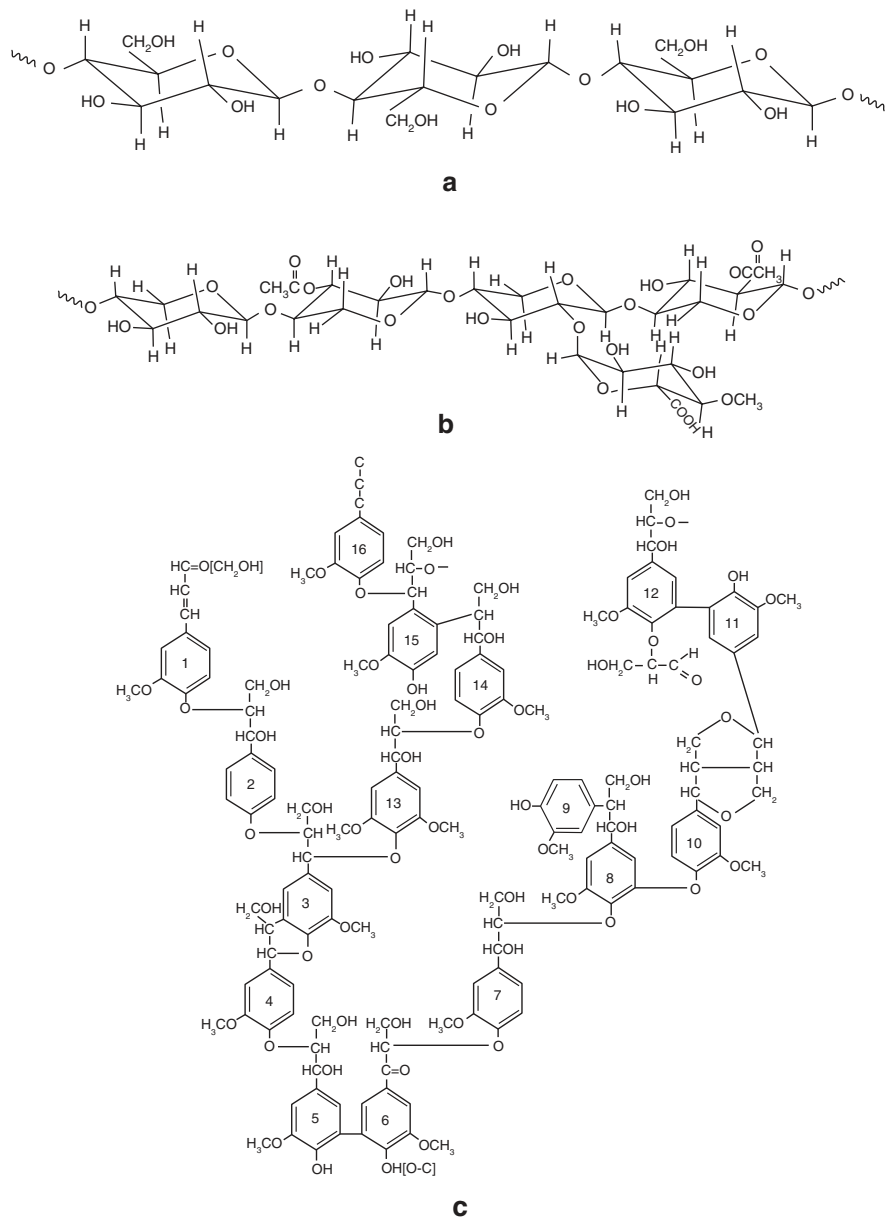


**Fig. 14.14** Repeating structures of cellulose (a), hemicellulose (b), and lignin (c). (From K.K. Pandey, Journal of Applied Polymer Science 1999, with permission of John Wiley and Sons. Lignin structure was reproduced from E. Alder (1977) with permission of Springer)

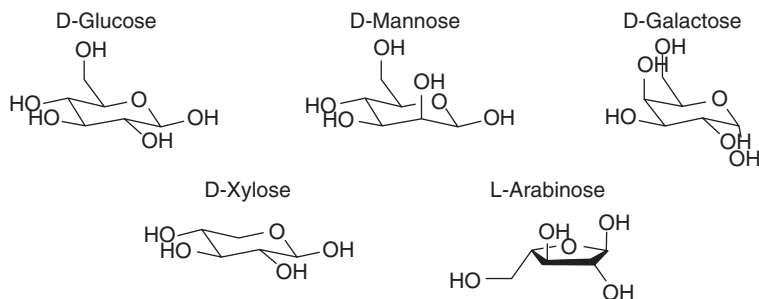


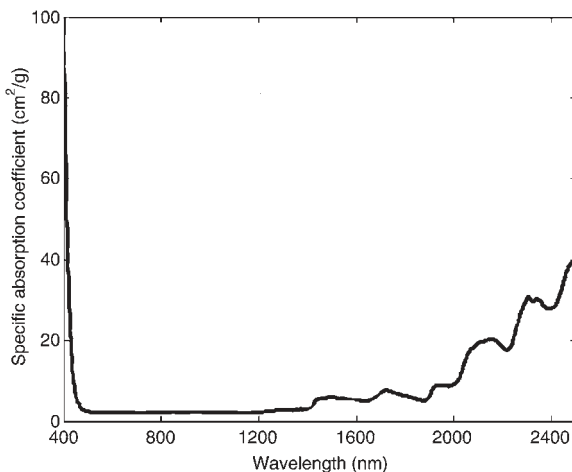
**Fig. 14.15** Examples of hemicellulose structures From Pierson et al. (2013), open access

(Curran 1989) and nearly impossible to untangle their spectral properties in intact leaves, at least with the spectral resolution and models available today. However, the variability in these properties makes it possible to use various regression, classification, and self-learning techniques to identify genera or species without knowing exactly the biochemical composition that identifies them. Features in the NIR and SWIR are relatively weak and spectrally broad, having originated as harmonics (integer multiples of the fundamental frequency) and overtones (frequencies higher than the fundamental frequency) from wavelengths in the UV and middle-infrared ranges (2500–6000 nm).

While the absorption spectra are not identical, cellulose, starch, and sugar have strong similarities due to their hydrocarbon chain chemical structures. The PROSPECT models continue to consider these compounds together as “dry matter content,” given the uncertainty in their absorption coefficients. Retrieval of dry matter in the models permits estimation of dry biomass; when expressed on a leaf area basis, this yields leaf mass area (dry biomass/leaf area), a measure shown to be highly correlated with photosynthetic production (Poorter et al. 2009). The presence or absence of various lignins, humic acids, and aromatic polyphenols can be determined from absorptions at 1420 and 1920 nm that are related to O–H bonds and C=O vibrations, with shoulders at 1700 and 2100 nm that are related to aromatic C–H bonds (Ziechmann 1964). Kokaly and Skidmore (2015) recently reported a narrow feature for aromatic C–H bonds in phenolic compounds of various woody species and non-hydroxylated aromatics at 1660 nm. Phenolic compounds are generally considered important in plant defense.

Curran (1989) noted that absorption features in leaves are broadened by multiple scattering and often interfere with one another. He cites an example where the first overtones of the N–H and O–H stretch overlap for most of their width. Thus, most studies have opted to analyze spectral data and relationships by identifying taxa or identifying leaf traits using various statistical methods such as multiple stepwise regression (e.g., Serrano et al. 2002), partial least squares regression (PLSR; e.g., Smith et al. 2002; Ollinger et al. 2008), discriminant function analysis (Filella et al. 1994), continuum removal (Kokaly and Clark 1999; Kokaly 2001), wavelets (Cheng et al. 2011, 2012, 2014; Kalacska et al. 2015), or a combination of PLSR, nested

**Fig. 14.16** Composite absorption coefficient for dry leaf chemistry used in the PROSPECT 4 and 5 model that was modified from earlier PROSPECT versions. Jacquemoud et al. (2000) and Féret et al. (2008), with permission from Elsevier



random effects—analysis of variance, and discriminant function analysis (Asner and Martin 2011; Asner et al. 2014b). Newer methods include Gaussian methods and various types of deep learning (Eches et al. 2011; Verrelst et al. 2012; Bazi et al. 2014; Sun et al. 2015). Some authors also combine leaf and canopy radiative transfer models with empirical models (e.g., Asner et al. 2014a, b; Gatellu-Etcheberry and Bruniquel-Pinel 2001). Féret et al. (2008), in developing PROSPECT 5, modified the specific absorption coefficient shown in Fig. 14.16 for dry matter (a composite representing the chemistry of dry leaves) based on a spectrum from Frederic Baret (CNES, unpublished) that Jacquemoud et al. (2009) tested against 245 dry leaves in the LOPEX93 database (Hosgood et al. 1995).

## 14.11 Conclusion

Researchers have sought to understand the optical properties of plant leaves for the past century or more. Great strides have been made in recent years, but much remains to be resolved before the full chemistry of leaves can routinely be determined from spectroscopy. This is a period of dynamic growth, at least partially because of the interdisciplinary research community—spanning physics, engineering, botany, ecology, RS, statistics, computer science, and modeling—that is interested in solving these problems. Much of the current interest originates from a desire to accurately quantify climate change impacts on global ecosystems, better understand global biodiversity patterns and their functional traits, find ways to monitor changes in global biodiversity, understand sustainability of production of natural and agricultural ecosystems, and better understand global biogeochemical cycles, specifically the C, N, and water budgets. Based on the number of papers estimating biodiversity and the methods applied, it is clear this is an active area of

research but also that we are still at the early stages of using optical features to determine alpha, beta, and gamma biodiversity and to develop robust measures for more completely understanding species mixtures and biodiversity.

## References

- Ackerly D (1999) Self-shading, carbon gain and leaf dynamics: a test of alternative optimality models. *Oecologia* 119:300–310
- Ackerly DD, Knight CA, Weiss SB, Barton K, Starmer KT (2002) Leaf size, specific leaf area and microhabitat distribution of chaparral woody plants: contrasting patterns in species level and community level analysis. *Oecologia* 130:449–457
- Adler E (1977) Lignin chemistry—past, present and future. *Wood Sci Technol* 11:169–218
- Al-Edany TY, Al-Saadi SAAM (2012) Taxonomic significance of anatomical characteristics in some species of the Family Myrtaceae. *Am J Plant Sci* 3:19475
- Allen WA, Gausman HW, Richards AJ, Wiegand CL (1970) Mean effective optical constants of 13 kinds of plant leaves. *Appl Opt* 9:2573. <https://doi.org/10.1364/AO.9.002573>
- Anderson ØM, Francis GW (2004) Techniques of pigment identification. *Plant pigments and their manipulation*. *Annu Plant Rev* 14:293–341
- Araus JL, Cairns JE (2014) Field high-throughput phenotyping: the new crop breeding frontier. *Trends Plant Sci* 19:52–61
- Arnold L, Gillet S, Lardiere O, Riaud P, Schneider J (2002) A test for the search for life on extrasolar planets. Looking for the terrestrial vegetation signature in the Earthshine spectrum. *Astron Astrophys* 392:231–237
- Asner GP, Martin RE (2011) Canopy phylogenetic, chemical and spectral assembly in a lowland Amazonian forest. *New Phytol* 189:999–1012
- Asner GP, Martin RE (2016) Spectranomics: emerging science and conservation opportunities at the interface of biodiversity and remote sensing. *Global Ecol Cons* 8:212–219
- Asner GP, Martin RE, Carranza-Jiménez L, Sinca F, Tupayachi R et al (2014a) Functional and biological diversity of foliar spectra in tree canopies throughout the Andes to Amazon region. *New Phytol* 204:127–139
- Asner GP, Martin RE, Tupayachi R, Anderson CB, Sinca F et al (2014b) Amazonian functional diversity from forest canopy chemical assembly. *Proc Natl Acad Sci U S A* 111:5604–5609
- Asner GP, Anderson CB, Martin RE, Tupayachi R, Knapp DE et al (2015) Landscape biogeochemistry reflected in shifting distributions of chemical traits in the Amazon forest canopy. *Nat Geosci* 8:567–573
- Bai G, Ge Y, Hussain W, Baenziger PS, Graef G (2016) A multi-sensor system for high throughput field phenotyping in soybean and wheat breeding. *Comput Electron Agr* 128:181–192
- Baranoski GVG, Eng D (2007) An investigation on sieve and detour effects affecting the interaction of collimated and diffuse infrared radiation (750–2500nm) with plant leaves. *IEEE Trans Geosci Remote S* 45:2593–2599
- Bazi Y, Alajlan N, Melgani F, Al Hichri H, Malek S (2014) Differential evolution extreme learning machine for the classification of hyperspectral images. *IEEE GeoSci Remote S* 11:1066–1070
- Beisel KG, Jahnke S, Hofmann D, Köppchen S, Schurr U, Matsubara S (2010) Continuous turnover of carotenenes and chlorophyll *a* in mature leaves of Arabidopsis revealed by <sup>14</sup>CO<sub>2</sub> pulse-chase labeling<sup>IOA</sup>. *Plant Physiol* 152:2188–2199
- Blankenship RE (2010) Early evolution of photosynthesis. *Plant Physiol* 154:434–438
- Bone RA, Lee DW, Norman JM (1989) Epidermal cells functioning as lenses in leaves of tropical rain-forest shade plants. *Appl Opt* 24:1408–1412
- Bubier JL, Moore TR, Bledzki LA (2007) Effects of nutrient addition on vegetation and carbon cycling in an ombrotrophic bog. *Glob Chang Biol* 13:1168–1186

- Buiteveld H, Hakvoort JMH, Donze M (1994) The optical properties of pure water. In: Jaffe JS (ed) SPIE, the International Society for Optical Engineering, Proc Ocean Opt XVII, vol 2258, pp 174–183
- Carter GA (1991) Primary and secondary effects of water content on the spectral reflectance of leaves. *Am J Bot* 78:916–924
- Cazzonelli C (2011) Carotenoids in nature: insights from plants and beyond. *Funct Plant Biol* 38(11):833–847
- Chalker-Scott L (1999) Environmental significance of anthocyanins in plant stress responses. *Phytochem Photobiol* 70:1–9
- Chapin FS, Autumn K, Pugnaire F (1993) Evolution of suites of traits in response to environmental stress. *Am Nat* 142(S):S78–S92
- Cheng T, Rivard B, Sanchez-Azofeifa AG (2011) Spectroscopic determination of leaf water content using continuous wavelet analysis. *Remote Sens Environ* 115:659–670
- Cheng T, Rivard B, Sanchez-Azofeifa AG, Féret JB, Jacquemoud S, Ustin SL (2012) Predicting leaf gravimetric water content from foliar reflectance across a range of plant species using continuous wavelet analysis. *J Plant Phys* 169:1134–1142
- Cheng T, Rivard B, Sanchez-Azofeifa AG, Féret JB, Jacquemoud S, Ustin SL (2014) Deriving leaf mass per area (LMA) from foliar reflectance across a variety of plant species using continuous wavelet analysis. *ISPRS J Photogramm Rem S* 87:28–38
- Comstock JP, Mahall BE (1985) Drought and changes in leaf orientation for two California shrubs: *Ceanothus megacarpus* and *Ceanothus crassifolius*. *Oecologia* 65:531–535
- Cooper GM, Hausman RE (2004) The chloroplast genome. In: Cooper GM, Hausman RE (eds) *The cell: a molecular approach*, 3rd edn. ASM Press, Washington, D.C., pp 417–418. ISBN 0878932143
- Couture JJ, Singh A, Rubert-Nason KF, Serbin SP, Lindroth RL, Townsend PA (2016) Spectroscopic determination of ecologically relevant plant secondary metabolites. *Methods Ecol Evol* 7:1402–1412
- Curcio JA, Petty CC (1951) The near infrared absorption spectrum of liquid water. *J Optical Soc Am* 41:302–304
- Curran PJ (1989) Remote sensing of foliar chemistry. *Remote Sens Environ* 30:271–278
- Demmig-Adams B, Gilmore AM, Adams WW III (1996) In vivo functions of carotenoids in higher plants. *FASEB J* 10:403–412
- Du H, Fuh RCA, Li J, Corkan LA, Lindsey JS (1998) PhotochemCAD: a computer-aided design and research tool in photochemistry. *Photochem Photobiol* 68:141–142
- Eches O, Dobigeon N, Tourneret JY (2011) Enhancing hyperspectral image unmixing with spatial correlations. *IEEE Trans Geosci Remote Sens* 49:4239–4247
- Ehleringer J, Björkman O, Mooney HA (1976) Leaf pubescence: effects on absorptance and photosynthesis in a desert shrub. *Science* 192:376–377
- Ellis RJ (1979) The most abundant protein in the world. *Trends Biochem Sci* 4:241–244
- Evans JR, Vogelmann TC, Williams WE, Gorton HL (2004) Chloroplast to leaf. In: Smith WC, Vogelmann TC, Critchley C (eds) *Photosynthetic adaptation: chloroplast to landscape*. Springer, New York, pp 15–41
- Everitt JH, Richardson AJ, Gausman HW (1985) Leaf reflectance-nitrogen-chlorophyll relations in buffelgrass. *Photogramm Eng Rem S* 5:463–466
- Féret J-B, Asner GP (2014a) Microtopographic controls on lowland Amazonian canopy diversity from imaging spectroscopy. *Ecol Appl* 24:1297–1310
- Féret J-B, Asner GP (2014b) Mapping tropical forest diversity using high-fidelity imaging spectroscopy. *IEEE Trans Geosci Remote S* 51:73–84
- Féret J-B, François C, Asner GP, Gitelson AA, Martin RE et al (2008) PROSPECT 4 and 5: advances in the leaf optical properties model separating photosynthetic pigments. *Remote Sens Environ* 112:3030–3043
- Féret J-B, François C, Gitelson A, Asner GP, Barry KM, Panigada C, Richardson AD, Jacquemoud S (2011) Optimizing spectral indices and chemometric analysis of leaf chemical properties using radiative transfer modeling. *Remote Sens Environ* 115:2742–2750

- Féret J-B, Gitelson AA, Noble SD, Jacquemoud S (2017) PROSPECT-D: towards modeling leaf optical properties through a complete lifecycle. *Remote Sens Environ* 193:204–215
- Field CB (1983) Allocating leaf nitrogen for the maximization of carbon gain – leaf age as a control on the allocation program. *Oecologia* 56:341–347
- Field CB, Mooney H (1986) The photosynthesis – nitrogen relationship in wild plants. In: Givnish TJ (ed) *On the economy of form and function*. Cambridge University Press, Cambridge, pp 25–55
- Filella I, Serrano L, Serra J, Peñuelas J (1994) Evaluating wheat nitrogen status with canopy reflectance indices and discriminant analysis. *Crop Sci* 35:1400–1405
- Fukshansky L, Martinez V, Remisowsky A, McClendon J, Ritterbusch A, Richter T et al (1993) Absorption spectra of leaves corrected for scattering and distributional error: a radiative transfer and absorption statistics treatment. *Photochem Photobiol* 57:538–555
- Gamon JA, Peñuelas J, Field CB (1992) A narrow-waveband spectral index that tracks diurnal changes in photosynthetic efficiency. *Remote Sens Environ* 41:35–44
- Gamon JA, Kovalchuck O, Wong CYS, Harris A, Garrity SR (2015) Monitoring seasonal and diurnal changes in photosynthetic pigments with automated PRI and NDVI sensors. *Biogeosciences* 12:4149–4159
- Gatellu-Etchegorry JP, Bruniquel-Pinel V (2001) A modeling approach to assess the robustness of spectrometric predictive equations for canopy chemistry. *Remote Sens Environ* 76:1–15
- Gates DM, Keegan HJ, Schleter JC, Weidner VR (1965) Spectral properties of plants. *Appl Opt* 4:11–20
- Gausman HW (1974) Leaf reflectance of near-infrared. *Photogramm Eng* 40:183–191
- Gitelson AA (2012) Nondestructive estimation of foliar pigment (chlorophylls, carotenoids, and anthocyanins) contents: evaluating a semi analytical three-band model. In: Thenkabail PS, Lyon JG, Huete A (eds) *Hyperspectral remote sensing of vegetation*. CRC Press-Taylor and Francis Group, Boca Raton; p 141–165
- Gras EK, Read J, Mach CT, Sanson GD, Clissold FJ (2005) Herbivore damage, resource richness and putative defenses in juvenile versus adult *Eucalyptus* leaves. *Aust J Bot* 53:33–44
- Haberlandt G (1914) *Physiological plant anatomy. Perception of light*. Macmillan and Co., London
- Hale GM, Querry MR (1973) Optical constants of water in the 200nm to 200µm wavelength region. *Appl Opt* 12:555–563
- Hamilton WD, Brown SP (2001) Autumn tree colours as a handicap signal. *Proc Royal Soc B-Biol Sci* 286(1475):1489–1493
- Hannoufa A, Houssain Z (2012) Regulation of carotenoid accumulation in plants. *Biocatal Agric Biotechnol* 1(3):198–202
- Hosgood B, Jacquemoud S, Andreoli G, Verdebout J, Pedrini G et al (1995) Leaf Optical properties EXperiment 93 (LOPEX93) report EUR-16095-EN. European Commission, Joint Research Centre, Institute for Remote Sensing Applications, Ispra
- Hrazdina G, Wagner GJ, Siegelman HW (1978) Subcellular localization of enzymes of anthocyanin biosynthesis in protoplasts. *Phytochemistry* 17:53–56
- Jacquemoud S, Ustin S (2008) Modeling leaf optical properties. *Photobiological Sciences Online. Environmental Photobiology*. <http://www.photobiology.info/#Environ>. Accessed 27 Nov 2018
- Jacquemoud S, Bacour C, Poilvé H, Frangi J-P (2000) Comparison of four radiative transfer models to simulate plant canopies reflectance: direct and inverse models. *Remote Sens Environ* 74:471–481
- Jacquemoud S, Verhoef W, Baret F, Bacour C, Zarco-Tejada PJ et al (2009) PROSPECT + SAIL models: a review of use for vegetation characterization. *Remote Sens Environ* 113(S1):S56–S66
- James SA, Bell DT (2000) Leaf orientation, light interception and stomatal conductance of *Eucalyptus globulus* ssp. *globulus* leaves. *Tree Physiol* 20:815–823
- Junker LV, Ensminger I (2016) Fast detection of leaf pigments and isoprenoids for ecophysiological studies, plant phenotyping and validating remote-sensing of vegetation. *Physiol Planta* 158:369–381

- Kalacska M, Lalonde M, Moore TR (2015) Estimation of foliar chlorophyll and nitrogen content in an ombrotrophic bog from hyperspectral data: scaling from leaf to image. *Remote Sens Environ* 169:270–279
- Karageorgou P, Manetas Y (2006) The importance of being red when young: anthocyanins and the protection of young leaves of *Quercus coccifera* from insect herbivory and excess light. *Tree Physiol* 26:613–621
- Kattge J, Diaz S, Lavelle S, Prentice IC, Leadley P et al (2011) TRY – a global database of plant traits. *Glob Chang Biol* 17:2905–2935
- Keles (2008) Liquid water absorption and refractive index. Compiled by Krebes (Created 1 July 2008), at English Wikipedia CC by SA 3.0 (<http://creativecommons.org/licenses/by-sa/3.0>). Based largely on publications by Segelstein (1981), Hale & Quarry (1973), and Wieliczka et al. (1989), but Krebes provides other references at: <http://omlc.ogi.edu/spectra/water/abs/index.html>. Accessed 18 Nov 2018
- Kiang NY, Siefert J, Govindjee, Blankenship RE (2007) Spectral signatures of photosynthesis. I. Review of earth organisms. *Astrobiology* 7:222–251
- Klemm D, Heublein B, Fink H-P, Bohn A (2005) Cellulose: fascinating biopolymer and sustainable raw material. *Angew Chem Int Edit* 44(22):3358–3393. <https://doi.org/10.1002/anie.200460587>
- Knipling EB (1970) Physical and physiological basis for the reflectance of visible and near-infrared radiation from vegetation. *Remote Sens Environ* 1:155–159
- Kokaly RF (2001) Investigating a physical basis for spectroscopic estimates of leaf nitrogen concentration. *Remote Sens Environ* 75:153–161
- Kokaly RF, Clark RN (1999) Spectroscopic determination of leaf biochemistry using band-depth analysis of absorption features and stepwise multiple linear regression. *Remote Sens Environ* 67:267–287
- Kokaly RF, Skidmore AK (2015) Plant phenolics and absorption features in vegetation reflectance spectra near 1.66 $\mu$ m. *Int J Appl Earth Observ Geoinform* 43:55–83
- Kokaly RF, Asner GP, Ollinger SV, Martin ME, Wessman CA (2009) Characterizing canopy biochemistry from imaging spectroscopy and its application to ecosystem studies. *Remote Sens Environ* 113:S78–S91
- Kou L, Labrie D, Chylek P (1993) Refractive indices of water and ice in the 0.65 to 2.5- $\mu$ m spectral range. *Appl Opt* 32:3531–3540
- Landi M, Tattini M, Gould KS (2015) Multiple functional roles of anthocyanins in plant-environment interactions. *Environ Exp Bot* 119:4–17
- Lee DW (2002) Anthocyanins in leaves: distribution, phylogeny and development. *Adv Bot Res* 37:37–53
- Lee DW, Collins TM (2001) Phylogenetic and ontogenetic influences on the distribution of anthocyanins and betacyanins in leaves of tropical plants. *Int J Plant Sci* 162:1141–1153
- Lee DW, Gould KS (2002) Anthocyanins in leaves and other vegetative organs: an introduction. *Adv Bot Res Incorporating Adv Plant Path* 37:1–16
- Li L, Zhang Q, Huang D (2014) A review of imaging techniques for plant phenotyping. *Sensors* 14:20078–20111. <https://doi.org/10.3390/s141120078>
- Lichtenthaler HK (1987) Chlorophylls and carotenoids: pigments of photosynthetic biomembranes. *Method Enzymol* 148:350–382
- Martin GM, Jossierand SA, Bornman JF, Vogelmann TC (1989) Epidermal focusing and the light environment within leaves of *Medicago sativa*. *Physiol Plant* 76:485–492
- Matile P (2000) Biochemistry of Indian summer: physiology of autumnal leaf coloration. *Exp Gerontol* 35:145–158
- Milborrow BV (2001) The pathway of biosynthesis of abscisic acid in vascular plants: a review of the present state of knowledge of ABA synthesis. *J Exp Bot* 52(359):1145–1164
- Montañés-Rodríguez P, Pallé E, Goode PR, Martin Tores FJ (2006) Vegetation signature in the observed globally integrated spectrum of earth considering simultaneous cloud data: applications for extrasolar planets. *Astrophys J* 651:544–552



- Mooney HA, Field C, Gulmon SL, Bazzaz FA (1981) Photosynthetic capacity in relation to leaf position in desert versus old-field annuals. *Oecologia* 50:109–112
- Ollinger S, Smith ML (2005) Net primary production and canopy nitrogen in a temperate forest landscape: an analysis using imaging spectroscopy, modeling and field data. *Ecosystems* 8:760–778
- Ollinger SV, Richardson AD, Martin ME, Hollinger DY, Froliking SE et al (2008) Canopy nitrogen, C assimilation, and albedo in temperate and boreal forests: functional relations and potential climate feedbacks. *Proc Natl Acad Sci U S A* 105:19336–19341
- Ordoñez JC, Van Bodegom PM, Witte J-P, Wright IJ, Reich PB et al (2009) A global study of relationships between leaf traits, climate and soil measures of nutrient fertility. *Global Ecol Biodiver* 18:137–149
- Owen NL, Thomas DW (1989) Infrared studies of “hard” and “soft” woods. *Appl Spectrosc* 43:451–455
- Palmer KF, Williams D (1974) Optical properties in the near infrared. *J Optical Soc Am* 64:1107–1110
- Pandy KK et al (1999) A study of chemical structure of soft and hardwood and wood polymers by FTIR spectroscopy. *J Appl Polym Sci* 71:1969–1975
- Parkhurst DF (1986) Internal leaf structure: a three-dimensional perspective. In: Givnish TJ (ed) *On the economy of plant form and function*. Cambridge University Press, Cambridge, pp 215–249
- Peters RD, Noble SD (2014) Spectrographic measurement of plant pigments from 300 to 800 nm. *Remote Sens Environ* 148:119–123
- Pierson Y, Bobbink F, Yan N (2013) Alcohol mediated liquefaction of lignocellulosic materials: a mini review. *Chem Eng Process Tech* 1(2):1014
- Poorter H, Niinemets Ü, Poorter L, Wright IJ, Villar R (2009) Causes and consequence of variation in leaf mass per area (LMA): a meta-analysis. *New Phytol* 182:565–588
- Poulson ME, Vogelmann TC (1990) Epidermal focusing and effects upon photosynthetic light-harvesting in leaves of *Oxalis*. *Plant Cell Environ* 13:803–811
- Raven JA (2013) Rubisco: still the most abundant protein on earth? *New Phytol* 198:1–3
- Roberts DA, Ustin SL, Ogunjemiyo S, Greenberg J, Dobrowski SZ, Chen J, Hinckley TM (2004) Spectral and structural measures of northwest forest vegetation at leaf to canopy scales. *Ecosystems* 7:545–562
- Schaepman-Strub G, Schaepman ME, Painter TH, Dangel S, Martonchik JV (2006) Reflectance quantities in optical remote sensing—definitions and case studies. *Remote Sens Environ* 103:28–42
- Segelstein D (1981) The complex refractive index of water. M.S. thesis, University of Missouri-Kansas City. Figure derived from Philip Laven [www.philiplaven.com/refractive](http://www.philiplaven.com/refractive) index of water. Accessed 7 Dec 2016
- Serbin SP, Singh A, Desai AR, Dubois SG, Jablonski AD et al (2015) Remotely estimating photosynthetic capacity, and its response to temperature, in vegetation canopies using imaging spectroscopy. *Remote Sens Environ* 167:78–87
- Serrano L, Peñuelas J, Ustin SL (2002) Remote sensing of nitrogen and lignin in Mediterranean vegetation from AVIRIS data: decomposing biochemical from structural signals. *Remote Sens Environ* 81:355–364
- Singh A, Serbin SP, McNeil BE, Kingdon CC, Townsend PA (2015) Imaging spectroscopy algorithms for mapping canopy foliar chemical and morphological traits and their uncertainties. *Ecol Appl* 25:2180–2197
- Smith WK, Vogelmann TC, DeLucia EH, Bell DT, Shepherd KA (1997) Leaf form and photosynthesis. *BioSci* 47:785–793
- Smith M-L, Ollinger SV, Martin ME, Aber JD, Hallett RA et al (2002) Direct estimation of above-ground forest productivity through hyperspectral remote sensing of canopy nitrogen. *Ecol Appl* 12:1286–1302
- Stapleton AE (1992) Ultraviolet radiation and plants: burning questions. *Plant Cell* 4:1353–1358

- Sterner RW, Elser JJ, Gorokhova E, Fagan WF, Markow TA et al (2002) Ecological stoichiometry: the biology of elements from molecules to the biosphere. Princeton University Press, Princeton, p 441
- Steyn WJ, Wand SJE, Holcroft DM, Jacobsm G (2002) Anthocyanins in vegetative tissues: a proposed unified function in photoprotection. *New Phytol* 155:349–361
- Sun S, Zhong P, Xiao HT, Wang RS (2015) Active learning with Gaussian process classifier for hyperspectral image classification. *IEEE Trans Geosci Remote Sens* 53:1746–1760
- Tanger P, Klassen S, Mojica JP, Lovell JT, Moyers BT et al (2017) Field-based high throughput phenotyping rapidly identifies genomic regions controlling yield components in rice. *Nature Sci Rep* 7:43839. <https://doi.org/10.1038/srep42839>
- Terashima I, Fujita T, Inoue T, Chow WS, Oguchi R (2009) Green light drives leaf photosynthesis more efficiently than red light in strong white light: revisiting the enigmatic question of why leaves are green. *Plant Cell Phys* 50:684–697
- Thayer SS, Björkman O (1990) Leaf xanthophyll content and composition in sun and shade determined by HPLC. *Photosyn Res* 23:331–343
- Thevenot M, Dignac M-F, Rumpel C (2010) Fate of lignins in soil: a review. *Soil Biol Biochem* 42:1200–1211
- Tilman D (1985) The resource-ratio hypothesis of plant succession. *Am Nat* 125:827–852
- Ustin SL, Gamon JA (2010) Remote sensing of plant functional types. *New Phytol* 186:795–816
- Ustin SL, Jacquemoud S, Govaerts Y (2001) Simulation of photon transport in a three-dimensional leaf: implications for photosynthesis. *Plant Cell Environ* 24:1095–1103
- Ustin SL, Gitelson AA, Jacquemoud S, Schaepman M, Asner GP, Gamon JA, Zarco-Tejada P (2009) Retrieval of foliar information about plant pigment systems from high resolution spectroscopy. *Remote Sens Environ* 113:S67–S77
- Ustin SL, Riaño D, Hunt ER Jr (2012) Estimating canopy water content from spectroscopy. *Israel J Plant Sci* 60:9–23
- Van Gaalen KE, Flagan LB, Peddle DR (2007) Photosynthesis, chlorophyll fluorescence and spectral reflectance in *Sphagnum* moss at varying water contents. *Oecologia* 153:19–28
- Vendramaini F, Díaz S, Gurvich DE, Wilson PJ, Thompson K et al (2002) Leaf traits as indicators of resource-use strategy in floras with succulent species. *New Phytol* 154:147–157
- Verrelst J, Camps-Valls G, Delegido J, Moreno J (2012) Retrieval of vegetation biophysical parameters using Gaussian process techniques. *IEEE Trans GeoSci Remote S* 50:1832–1843
- Vogelmann TC (1993) Plant tissue optics. *Annu Rev Plant Phys* 44:231–251
- Vogelmann JR, Moss DM (1993) Spectral reflectance measurements in the genus *Sphagnum*. *Remote Sens Environ* 45:273–279
- Vogelmann TC, Nishio JN, Smith WK (1996a) Leaves and light capture: light propagation and gradients of carbon fixation within leaves. *Trends Plant Sci* 1:65–71
- Vogelmann TC, Bornman JF, Yates DJ (1996b) Focusing of light by leaf epidermal cells. *Physiol Plant* 98:48–56
- Weng J-K, Chapple C (2010) The origin and evolution of lignin biosynthesis. *New Phytol* 187:273–285
- Wieliczka DM, Weng SS, Querry MR (1989) Wedge shaped cell for highly absorbent liquids – infrared optical – constants of water. *Appl Opt* 28:1714–1719
- Wooley JT (1971) Reflectance and transmittance of light by leaves. *Plant Physiol* 47:656–662
- Wooley JT (1975) Refractive index of soybean leaf cell walls. *Plant Physiol* 55:172–174
- Workman J Jr, Weier L (2012) Practical guide and spectral atlas for interpretative infrared spectroscopy. Francis and Taylor Group, Boca Raton
- Wright IJ, Reich PB, Westerby M, Ackerly DD, Baruch Z et al (2004) The worldwide leaf economics spectrum. *Nature* 428:821–827
- Wright IJ, Reich PB, Cornelissen JHC, Falster DS, Groom PK et al (2005) Modulation of leaf economic traits and trait relationships by climate. *Global Ecol Biogeo* 14:411–421
- Ziehm W (1964) Spectroscopic investigations of lignin, humic substances and peat. *Geochim Cosmochim Acta* 28:1555–1566

**Open Access** This chapter is licensed under the terms of the Creative Commons Attribution 4.0 International License (<http://creativecommons.org/licenses/by/4.0/>), which permits use, sharing, adaptation, distribution and reproduction in any medium or format, as long as you give appropriate credit to the original author(s) and the source, provide a link to the Creative Commons license and indicate if changes were made.

The images or other third party material in this chapter are included in the chapter's Creative Commons license, unless indicated otherwise in a credit line to the material. If material is not included in the chapter's Creative Commons license and your intended use is not permitted by statutory regulation or exceeds the permitted use, you will need to obtain permission directly from the copyright holder.

